

Lecce University LE/ASTRO 3/96  
Pavia University FNT/T-96/16  
Zurich University ZU-TH 8/96

## Halo Dark Clusters of Brown Dwarfs and Molecular Clouds

F. De Paolis<sup>1,2</sup>, G. Inghrosso<sup>3</sup>, Ph. Jetzer<sup>2</sup> and M. Roncadelli<sup>4,\*</sup>

<sup>1</sup> Bartol Research Institute, University of Delaware, Newark, Delaware, 19716-4793, USA

<sup>2</sup> Paul Scherrer Institut, Laboratory for Astrophysics, CH-5232 Villigen PSI, and Institute of Theoretical Physics, University of Zurich, Winterthurerstrasse 190, CH-8057 Zurich, Switzerland

<sup>3</sup> Dipartimento di Fisica, Università di Lecce, Via Arnesano, CP 193, 73100 Lecce, Italy

and INFN, Sezione di Lecce, Via Arnesano, CP 193, 73100 Lecce, Italy

<sup>4</sup> INFN, Sezione di Pavia, Via Bassi 6, I-27100, Pavia, Italy

### Abstract

The discovery of Massive Astrophysical Compact Halo Objects (MACHOs) in microlensing experiments makes it compelling to understand their physical nature, as well as their formation mechanism. Within the present uncertainties, brown dwarfs are a viable candidate for MACHOs, and the present paper deals with this option. According to a recently proposed scenario, brown dwarfs are clumped along with cold molecular clouds into dark clusters – in several respects similar to globular clusters – which form in the outer part of the galactic halo. Here, we analyze the dynamics of these dark clusters and we address the possibility that a sizable fraction of MACHOs can be binary brown dwarfs. Moreover, we point out that Ly- $\alpha$  absorption systems naturally fit within the present picture.

Subject headings: Dark matter - Galaxy: halo - Galaxy: kinematics and dynamics - Gravitational microlensing

\* Work partially supported by Dipartimento di Fisica Nucleare e Teorica, Università di Pavia, Pavia Italy

# 1 Introduction

Observations of microlensing events (Alcock et al. [1993], Aubourg et al. [1993]) towards the Large Magellanic Cloud (LMC) strongly suggest that a substantial fraction of the galactic halo should be in the form of dark compact objects, named MACHOs (massive astrophysical compact halo objects) (De Rújula, Jetzer and Massò [1992]).

Actually, the MACHO collaboration has recently announced the discovery of several new events during their second year of observations (Alcock et al. [1997]), and 8 microlensing events have been detected so far <sup>1</sup>.

Although the presently-available limited statistics prevents clear-cut conclusions to be drawn from experimental data (Gates, Gyuk and Turner [1996]), the evidence for such a discovery is firm and its implications are striking. In fact – under the assumption that MACHOs are indeed located in the galactic halo – the inferred halo mass in MACHOs within 50 kpc turns out to be  $2.0_{-0.7}^{+1.2} \times 10^{11} M_{\odot}$  (Alcock et al. [1997]), which is several times larger than the mass of all known stellar components of the Galaxy and represents a relevant portion of the galactic dark matter. Remarkably enough, this result is almost independent of the assumed galactic model. Unfortunately, this circumstance contrasts with the strong model-dependence of the average MACHO mass. It has become customary to take the standard spherical halo model as a baseline for comparison. Regretfully – because of the low statistics – different data-analysis procedures lead to results which are only marginally consistent. Specifically, within the standard halo model, the average MACHO mass reported by the

---

<sup>1</sup>It should be mentioned that the MACHO team has found at least seven more events (which are reported on the Alert list), but a full analysis of them has not yet been published.

MACHO team is  $0.46_{-0.2}^{+0.3} M_{\odot}$  (Alcock et al. [1997]), whereas the mass moment method (De Rújula, Jetzer and Massó [1991]) yields  $0.27 M_{\odot}$  (Jetzer [1996]).

What can be reliably concluded from the existing data-set is that MACHOs should lie in the mass range  $0.05 - 1.0 M_{\odot}$  (see also Table 9 in Alcock et al. [1997]), but stronger claims are unwarranted because of the high-sensitivity of the average MACHO mass on the uncertain properties of the considered galactic model (Evans [1996], De Paolis, Ingrassio and Jetzer [1996]).

Mass values  $> 0.1 M_{\odot}$  suggest that MACHOs should be either M-dwarfs or else white dwarfs. Observe that these mass values naturally arise within the standard halo model.

As a matter of fact, deeper considerations show that the M-dwarf option can look problematic. The null results of several searches for low-mass stars both in the disk and in the halo of our galaxy (Hu et al. [1994]) entail that the halo cannot be mostly in the form of hydrogen-burning main-sequence M-dwarfs. Optical imaging of high-latitude fields taken with the Wide Field Camera of the Hubble Space Telescope indicates that less than  $\sim 6\%$  of the halo mass can be in this form (Bahcall et al. [1994]). A more detailed analysis which accounts for the fact that halo stars likely have a lower metallicity (with respect to the solar one) leads to an even more stringent upper limit of less than  $\sim 1\%$  (Graff and Freese [1996]). We emphasize that these results are derived under the assumption of a smooth spatial distribution of M-dwarfs, and become less severe in the case of a clumpy distribution (Kerins [1996]). In the latter case, as pointed out by Kerins [1997], the dynamical limits and HST observations require that the overwhelming fraction of M-dwarfs, at least 95%, must still reside in clusters at present. His analysis shows that there exists a wide range

of cluster masses and radii which are consistent with these requirements.

As we said, an alternative explanation for MACHOs can be provided – within the standard spherical halo model – by white dwarfs, and a scenario with white dwarfs as a major constituent of the galactic halo dark matter has been explored (Tamanaha et al. [1990], Fields et al. [1996], Adams and Laughlin [1996], Chabrier, Segretain and Méra [1996]). However, even this proposal meets difficulties. Besides requiring a rather *ad hoc* initial mass function (IMF) of the progenitor stars sharply peaked somewhere in the range  $1 - 8 M_{\odot}$  and a halo age larger than  $\sim 16$  Gyr, strong constraints on the number density of halo white dwarfs arise from present-day metal abundances in the interstellar medium (Ryu, Olive and Silk [1990], Gibson and Mould [1996]) and from deep galaxy counts (Charlot and Silk [1995]). In any case, future HST deep field exposures will either find the white dwarfs or put constraints on their fraction in the halo (Kawaler [1996]).

Mass values  $\lesssim 0.1 M_{\odot}$  make brown dwarfs <sup>2</sup> an attractive candidate for MACHOs <sup>3</sup>. In fact, these mass values are supported by several nonstandard halo models. An example is provided by the maximal disk model (van Albada & Sancisi [1986]; Persic & Salucci [1990]; Sackett [1996]), in which more matter is comprised within the disk whereas the halo is less massive as compared with the standard halo model. The latter fact implies a falling rotation curve, and so a smaller transverse velocity of MACHOs. Hence, the microlensing time scale gets longer for a given MACHO mass, which means a smaller implied MACHO mass

---

<sup>2</sup>Brown dwarfs have been discovered quite recently in the solar neighbourhood and in the Pleiades cluster (Rebolo et al. [1995], Nakajima et al. [1995]). The idea that MACHOs are brown dwarfs has been contemplated by several authors (see Carr [1994] and references therein).

<sup>3</sup>We notice that the limit for hydrogen burning – usually quoted as  $0.08 M_{\odot}$  – gets increased up to  $0.11 M_{\odot}$  for low-metallicity objects, such as a halo population (D’Antona [1987], Burrows, Hubbard & Lunine [1989]).

for a given observed timescale. We stress that a reduced transverse velocity of MACHOs arises also in other nonstandard halo models. For instance, a radially anisotropic velocity distribution or a halo rotation would do the job (Alcock et al. [1997]; Evans [1996]; De Paolis, Ingrosso & Jetzer [1996]). We also notice that the EROS collaboration (Renault et al. [1997]) has shown that MACHOs in the mass range  $10^{-7} - 2 \times 10^{-2} M_{\odot}$  do not contribute significantly (less than 20%) to the halo dark matter (this result is consistent with the MACHO experiment for objects of mass  $0.1M_{\odot}$  to  $1M_{\odot}$ ).

Although present uncertainties do not permit to make any sharp statement about the nature of MACHOs, brown dwarfs still look as a viable possibility to date, and we shall stick to it throughout.

Even if MACHOs are indeed brown dwarfs, the problem nevertheless remains to explain their formation, as well as the nature of the remaining dark matter in galactic halos.

We have previously proposed a scenario in which dark clusters of brown dwarfs and cold molecular clouds – mainly of  $H_2$  – naturally form in the halo at galactocentric distances larger than 10 – 20 kpc (De Paolis et al. [1995a]-[1995d]). Similar ideas have also been put forward by Gerhard and Silk [1996]. A slightly different picture based on the presence of a strong cooling-flow phase during the formation of our galaxy has been considered by Fabian and Nulsen [1994, 1997] and leads to a halo made of low-mass objects. In addition, Pfeniger, Combes and Martinet [1994] suggested that  $H_2$  clouds can constitute the dark matter in the disk of our galaxy.

The model in question encompasses the one first proposed by Fall and Rees [1985] to explain the formation of globular clusters, and no substantial additional

hypothesis is required. Various resulting observational implications have also been addressed. In particular

*i*) the  $\gamma$ -ray flux arising from halo molecular clouds through the interaction with high-energy cosmic-ray protons has been estimated (De Paolis et al. [1995a, 1995b]);

*ii*) an anisotropy in the Cosmic Background Radiation (CBR) is predicted to show up when looking at the halo of M31 galaxy (De Paolis et al. [1995c]);

*iii*) the infrared emission from MACHOs located in the halo of M31 galaxy turns out to be observable with the detector on ISO satellite or with the next generation of satellite-borne detectors (De Paolis et al. [1995c]).

We would like to stress that a large amount of MACHOs – up to 50% in mass – can well consist of binary brown dwarfs, formed either by the same fragmentation process that produces individual brown dwarfs or later when the dark clusters start to undergo core collapse.

The aim of the present paper is to discuss in a systematic fashion further aspects of the above scenario. Basically, we try to figure out the dynamics of dark clusters. More specifically, we investigate the constraints which ensure their survival against various kinds of gravitational perturbations. In addition, we demonstrate that – because of dynamical friction on molecular clouds in the dark cluster cores (to be referred to as *frictional hardening*) – the present orbital radius of not too hard binary brown dwarfs turns out to be typically of the order of the Einstein radius for microlensing towards the LMC. As a consequence, taking also into account the adopted selection procedure in the data analysis, we understand why they have not been resolved so far – still, we argue that they can be resolved in future microlensing experiments with a

more accurate photometric observation. Finally, we show that Ly- $\alpha$  absorption systems naturally fit within our model.

The plan of the paper is as follows. In Section 2 we recall the main points of the considered picture for the formation of dark clusters. Various dynamical constraints are thoroughly analyzed in Section 3, paying particular attention to the phenomenon of core collapse. In Section 4 we study the process whereby brown dwarfs form close binary systems (as a consequence of core collapse) and we investigate the mechanism of frictional hardening in great detail. In Section 5 we turn our attention to the thermal balance in the halo molecular clouds. Section 6 contains a short discussion of the relevance of Ly- $\alpha$  absorption systems for the present scenario. Our conclusions are offered in Section 7.

## 2 Scenario for dark cluster formation

As shown elsewhere (De Paolis et al. [1995a, 1995b]), the model in question encompasses the one first considered by Fall and Rees [1985] for the formation of globular clusters <sup>4</sup> and relies upon the result of Palla, Salpeter and Stahler [1983] (hereafter PSS) that the lower bound on the Jeans mass in a collapsing metal poor cloud can be as low as  $10^{-2}M_{\odot}$ , provided certain environmental conditions are met.

Let us begin by summarizing the ideas of Fall and Rees [1985] from a point of view which is most convenient for our considerations.

After the initial collapse, the proto galaxy (PG) is expected to reach a quasi-hydrostatic equilibrium state with virial temperature  $\sim 10^6$  K. Fall and Rees

---

<sup>4</sup>A somewhat different extension of the Fall and Rees [1985] scheme has been proposed by Ashman [1990]. Among his motivations was the large spread in the age of globular clusters found by Larson [1990]. However, it seems nowadays that the stars in the halo of our galaxy have a small scatter in ages (Unavane, Wyse and Gilmore [1996]).

[1985] have shown that in such a situation a thermal instability develops: density enhancements rapidly grow as the gas cools to lower temperatures. In fact, irregularities in the inflow during the gas collapse and also fluctuations in the distribution of nonbaryonic dark matter (if present on the galactic scale) would introduce perturbations with a wide range in size and amplitude. As a result, randomly distributed overdense regions will form inside the PG. For reasons that will become clear later, these overdense regions will be referred to as proto globular cluster (PGC) clouds.

Under the assumption that the plasma in the PG is in collisional ionization equilibrium, it turns out that the cooling rate (as a function of density  $\rho$  and temperature  $T$ ) has the form

$$\Lambda(\rho, T) = \rho^2 L(T) \quad (1)$$

(the expression of  $L(T)$  can be found e.g. in Einaudi and Ferrara [1991]). The cooling time is

$$t_{cool} = \frac{3\rho k_B T}{2\mu(\Lambda - \Gamma)}, \quad (2)$$

where the heating rate  $\Gamma$  due to external heating sources has been taken into account (here  $\mu \simeq 1.22 m_p$  is the mean molecular mass of the primordial gas). Since at the high temperatures under consideration the heating rate can safely be neglected, it follows that  $t_{cool} \sim \rho^{-1}$ . On the other hand, the free-fall time reads

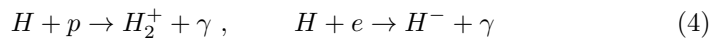
$$t_{ff} \sim (G\rho)^{-1/2}, \quad (3)$$

and so we see that  $t_{cool}$  decreases faster than  $t_{ff}$  as  $\rho$  increases. As the above quasi-hydrostatic equilibrium state of the PG is characterized by the condition  $t_{cool} \sim t_{ff}$ , it is clear that inside the PGC clouds we have  $t_{cool} < t_{ff}$ . That is

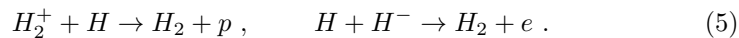


to say, the PGC clouds cool more rapidly than the rest of the PG. This process continues until hydrogen recombination occurs, because as soon as this happens – at a temperature  $\sim 10^4$  K – the cooling rate decreases precipitously, under the ionization equilibrium assumption (Dalgarno and McCray [1972]). Therefore, the regime  $t_{cool} > t_{ff}$  should now be established even in the PGC clouds and so the PG can be regarded at this stage as a two-phase medium, with cold PGC clouds in pressure equilibrium with the external (inter PGC clouds) diffuse hot gas.

However, Kang et al. [1990] realized that the fast radiative cooling of the PGC clouds (from  $10^6$  K to  $10^4$  K) implies that the plasma inside these clouds cools more rapidly than it recombines, so that the above ionization equilibrium assumption is violated. Actually, the out-of-equilibrium recombination results in an enhanced ionization fraction. This fact does not affect the previous conclusions for temperatures  $> 10^4$  K, but entails drastic changes at lower temperatures. Indeed, the existence of a sizable amount of protons and electrons at temperatures  $< 10^4$  K gives rise to  $H_2$  formation via the following reactions <sup>5</sup>



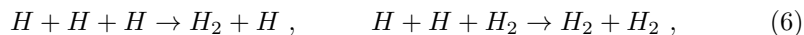
and



As a consequence, the PGC clouds undergo a further cooling below  $10^4$  K. Specifically, there is a direct radiative cooling via reactions (4) and a radiative cooling via excitation of roto-vibrational transitions of  $H_2$  (observe that  $H_2$  is further produced by reactions (5) and (6) below). We stress that the latter

<sup>5</sup>We wish to emphasize that the familiar reaction  $H + H \rightarrow H_2 + \gamma$  (which requires grains in order to be efficient) is presently irrelevant, since no dust exists in the metal poor PGC clouds.

process is very effective (much more than the former) at temperatures  $< 10^4$  K and plays a crucial rôle in our considerations. Since now  $t_{cool} \ll t_{ff}$  in the PGC clouds, the collapse goes on and the PGC cloud density rises steadily. When the number density in the PGC clouds exceeds  $10^8 \text{ cm}^{-3}$ , the  $H_2$  production increases dramatically thanks to the three-body reactions



as pointed out by PSS. In effect, these reactions are so efficient that virtually all the atomic hydrogen gets rapidly converted <sup>6</sup> to  $H_2$ . Correspondingly, the cooling of the PGC clouds is strongly enhanced and their evolution can proceed as in the scenario proposed by PSS.

Still, it goes without saying that  $H_2$  can be dissociated by various sources of ultraviolet (UV) radiation, like an active galactic nucleus (AGN) or a population of massive young stars (population III, see Carr, Bond and Arnett [1984]) at the centre of the PG. So, the ultimate fate of the PGC clouds strongly depends – apart from other environmental conditions (more about this, later) – on the survival of  $H_2$ .

In the early phase of the PG an AGN is expected to form at its centre along with population III stars, because of the disruption of central PGC clouds. This indeed happens, for the cloud collision time is shorter than the cooling time in the central region of the PG.

Thus,  $H_2$  will be dissociated at galactocentric distances smaller than a certain critical value  $R_{crit}$ . Following the analysis of Kang et al. [1990], it is straightforward to evaluate  $R_{crit}$ . Consider first the case of a UV flux due to a

---

<sup>6</sup>Observe that – at variance with reactions (4) and (5) – reactions (6) do not require the presence of electrons and protons as a catalyst.

central AGN. Then we find

$$R_{crit}^{AGN} \simeq \left( \frac{L_{AGN}}{2 \times 10^{42} \text{ erg s}^{-1}} \right)^{1/2} \text{ kpc} . \quad (7)$$

For typical luminosities up to  $L_{AGN} \simeq 10^{45} \text{ erg s}^{-1}$ , eq. (7) yields  $R_{crit}^{AGN} \simeq 20$  kpc. On the other hand, when the UV dissociating flux is produced by massive young stars mainly located at the centre of the PG, the critical galactocentric distance turns out to be

$$R_{crit}^* \simeq \left( \frac{10^{-3} \text{ kpc}^{-3}}{n_0} \right) \left( \frac{L_{tot}}{L_*} \right) \text{ kpc} . \quad (8)$$

In eq. (8)  $L_* \simeq 2 \times 10^{38} \text{ erg s}^{-1}$  is the bolometric luminosity of a single B0 V star. Assuming a total stellar luminosity  $L_{tot}$  up to  $\simeq 2 \times 10^{45} \text{ erg s}^{-1}$  and a central number density  $n_0$  up to  $\simeq 10^3 \text{ kpc}^{-3}$ , we find  $R_{crit}^* \simeq 10$  kpc. In conclusion,  $H_2$  should remain undissociated at galactocentric distances larger than 10 – 20 kpc.

## 2.1 Globular clusters

According to the foregoing analysis, in the inner galactic halo – that is for galactocentric distances smaller than 10 – 20 kpc –  $H_2$  gets dissociated <sup>7</sup>, thus preventing any further cooling of the PGC clouds below  $T \sim 10^4$  K. Therefore, these clouds remain for a long time in quasi-hydrostatic equilibrium at  $T \sim 10^4$  K (namely we have  $t_{cool} > t_{ff}$  during this period). In such a situation a characteristic mass scale gets imprinted on the PGC clouds by the gravitational instability, thereby resulting in a strongly peaked mass spectrum of the PGC clouds. In fact, Fall and Rees [1985] have shown that the Jeans mass of the

<sup>7</sup>This indeed occurs for a wide range of UV fluxes and PGC cloud densities (Kang et al. [1990]).

PGC clouds after the long permanence at  $T \sim 10^4$  K is given (as a function of the galactocentric distance  $R$ ) by <sup>8</sup>

$$M_{PGC}(R) \simeq 5 \times 10^5 (R/\text{kpc})^{1/2} M_{\odot} , \quad (9)$$

while the PGC radius turns out to be

$$r_{PGC}(R) \simeq 20 (R/\text{kpc})^{1/2} \text{ pc} . \quad (10)$$

Observe that in the present case the propagation of sound waves erases all large-scale perturbations, leaving only those at small scales.

Surely, this is not the end of the story, since the UV flux is expected to eventually decrease. So, after some time a nontrivial fraction of  $H_2$  should anyway form, causing a sudden drop of the PGC cloud temperature well below  $\sim 10^4$  K (the clouds now enter the regime  $t_{cool} < t_{ff}$ ). What next happens is a rapid growth of the small-scale perturbations, which lead directly (in one step) – due to the thermal instability – to formation of stars inside the PGC clouds (Murray and Lin [1989]). It goes without saying that we expect supernova explosions to have occurred, thus giving rise to shocks inside globular clusters and, therefore, leading to a rather wide stellar IMF. In this way, globular clusters should form as they are observed today especially in the inner part of the galactic halo. Incidentally, the formation of the PGC clouds could have been delayed until after the Galaxy was enriched by metals due to population III stars, in this manner explaining the absence of globular clusters with primordial metal abundances and the radial gradient of metallicity in the galactic halo.

---

<sup>8</sup>We stress that the  $R$ -dependence in eqs. (9) and (10) holds for  $R < 20$  kpc only (see the discussion in Vietri and Pesce [1995]), while for  $R > 20$  kpc the mass of globular clusters tends rather to decrease.

## 2.2 Dark clusters of MACHOs and cold molecular clouds

As we have seen, in the outer galactic halo – namely for galactocentric distances larger than 10 – 20 kpc –  $H_2$  molecules are not dissociated due to the absence of a significant UV flux. Under the assumption of a quiet environment, this circumstance entails a very efficient cooling of the PGC clouds, whose state is therefore characterized by the condition  $t_{cool} < t_{ff}$ . Hence, the gravitational collapse is expected to occur as in the scenario of PSS. Specifically, both the temperature decrease and the density increase cause a substantial drop of the Jeans mass for the PGC clouds. As a consequence, they fragment into smaller and smaller clouds. This process stops when the clouds become optically thick to their own radiation, since then cooling manifestly gets ineffective. PSS have shown that such a situation occurs when the Jeans mass is as low as  $10^{-2} M_{\odot}$ . We remark that the presence of rotation and magnetic fields in the PGC clouds would allow the Jeans mass to drop even further. Obviously, the fragmentation down to low-mass values is favoured if the initial gas has been metal enriched by population III stars (see Figure 7 in Palla and Stahler [1988]).

The result of the above picture is the formation of dark clusters containing compact objects with an IMF peaked in the range  $10^{-2} - 10^{-1} M_{\odot}$ . This value is close to the peak mass  $\sim 0.1 M_{\odot}$  of the present day IMF in the disk (Miller and Scalo [1979]), but in our case we expect it to decrease much more rapidly for higher masses and thus to be more narrow around its mean value. So, the compact objects in question should be predominantly brown dwarfs, even though a fraction of M-dwarfs can be present. Actually, we want to stress that our considerations still hold true even if a large fraction of MACHOs consists of M-

dwarfs <sup>9</sup> (as already mentioned, Kerins [1997] has shown that M-dwarfs clumped into clusters is a viable possibility to date). Notice that the expected lower limit of  $\sim 10^{-2} M_{\odot}$  is consistent with present bounds coming from microlensing data, as found by the EROS collaboration (Renault et al. [1997]).

What are the environmental conditions (besides  $H_2$  survival) which permit the mechanism in question to work? First, turbulence should be negligible. Indeed, turbulence effects would make fragments collide and – as shown by PSS – this fact would increase the Jeans mass. Second, no sizable gravitational perturbations (shocks, supernova explosions, etc.) should be present <sup>10</sup>, for otherwise they would induce the gravitational collapse before cooling has succeeded in lowering the fragment Jeans mass down to the above-mentioned values. Because these environmental conditions are likely to have occurred in the outer halo, the mass of the produced compact objects is expected to be close to the corresponding Jeans mass.

Besides individual brown dwarfs, it seems quite natural to suppose that – much in the same way as it happens for ordinary stars – also in this case the fragmentation process should produce a substantial fraction of binary brown dwarfs. For reasons that will become clear later, they will be referred to as *primordial* binaries (we shall come back to this issue in the next Sections). It is important to keep in mind that the mass fraction of primordial binaries can be as large as 50% (Spitzer and Mathieu [1980]).

So, we are led to the conclusion that MACHOs consist of both individual

---

<sup>9</sup>The reader should keep this point in mind, in spite of our talking about brown dwarfs. Of course, quantitative changes in some results will occur, because M-dwarfs are more massive than brown dwarfs (this is especially true concerning Sects. 3 and 4).

<sup>10</sup>This circumstance is consistent with our assumption that the stellar IMF in the dark clusters is more sharply peaked than the IMF in the globular clusters and in the disk.

and binary brown dwarfs in this scenario (more about this, later).

However, we don't expect the fragmentation process to be able to convert the whole gas in a PGC cloud into brown dwarfs. For instance, standard stellar formation mechanisms lead to an upper limit of at most 40% for the conversion efficiency (Scalo [1985]). Therefore, a fairly large amount of gas – mostly  $H_2$  – should have been left over. What is its fate? At variance with the case of globular clusters, strong stellar winds are now manifestly absent, and so this gas should remain gravitationally bound in the dark clusters. Actually, this conclusion is further supported by the following arguments (provided dark clusters comprise a consistent fraction of the galactic dark matter). First, the gas cannot have diffused into the whole halo, for otherwise it would have been heated by the gravitational field to a virial temperature  $\sim 10^6$  K, thereby becoming observable in the X-ray band – this option is ruled out by the available upper limits (Dickey and Lockman [1990])<sup>11</sup>. Second, the alternative possibility that the gas wholly collapsed into the disk is also excluded, because the disk mass would then be of the order of the inferred dark halo mass. Now, the virial theorem entails that the temperature  $T_{DG}$  of a *diffuse* gas component inside a dark cluster is

$$T_{DG} \simeq 1.1 \left( \frac{M_{DC}}{M_\odot} \right)^{2/3} \text{ K} . \quad (11)$$

Accordingly, a large fraction of diffuse gas would presumably give rise to an unobserved radio emission. Thus, we conclude that the amount of virialized diffuse gas inside a dark cluster has to be low (it will henceforth be neglected).

This circumstance implies in turn that most of the leftover gas should be in the form of *self-gravitating* clouds clumped into the dark clusters (since in this case

<sup>11</sup>Incidentally, the same argument also rules out a halo primarily made of *unclustered* brown dwarfs (as well as white and M-dwarfs).

the virial theorem applies to individual clouds). As we shall see later, there are good reasons to believe that the central temperature  $T_m$  of the molecular clouds in question should be very low, in fact close to that of the CBR. Accordingly, the molecular cloud mass  $M_m$  and median radius  $r_m$  are related by the virial theorem as

$$r_m \simeq 4.8 \times 10^{-2} \left( \frac{M_m}{M_\odot} \right) \text{ pc} . \quad (12)$$

Presumably, the fraction of cluster dark matter in the form of molecular clouds should be a function of the galactocentric distance  $R$ , depending on the environmental conditions, like the UV flux and the collision rate for the PGC clouds.

Before proceeding further, an important issue should be faced. Given the supposed existence of a large amount of gas in the dark clusters, one would expect a star formation process to be presently operative. However, things are not so simple. For – under the above environmental conditions – only stars with mass smaller than the cloud mass can be formed. Evidently, these stars are again either brown dwarfs or M-dwarfs. So, we see that undetected bright stars should not form in the dark clusters to the extent that our assumptions hold true. One might also wonder whether a sizable amount of gas is eventually left over. As already pointed out, we argue that this should be the case, for otherwise it would mean that the brown or M-dwarf formation mechanism should be much more efficient than any known star formation mechanism. Moreover, Gerhard and Silk [1996] have shown that the cluster gravitational field can stabilize the clouds against collapse.

Unfortunately, the lack of any observational information about dark clusters would make any effort to understand their structure and dynamics hopeless,



were it not for some remarkable insights that our unified treatment of globular and dark clusters provides us.

In the first place, it looks quite natural to assume that also dark clusters have a denser core surrounded by an extended spherical halo. For simplicity, we shall suppose throughout that the core density profile can be taken as constant. Moreover, it seems reasonable to imagine (at least tentatively) that dark clusters have the same average mass density as globular clusters. Hence, we obtain

$$r_{DC} \simeq 0.12 \left( \frac{M_{DC}}{M_{\odot}} \right)^{1/3} \text{ pc}, \quad (13)$$

where  $M_{DC}$  and  $r_{DC}$  denote the mass and the median radius of a dark cluster, respectively. In addition, dark clusters – just like globular clusters – presumably stay for a long time in a quasi-stationary phase, with an average central density  $\rho_*(0)$  slightly lower than  $10^4 M_{\odot} \text{ pc}^{-3}$  (which is the observed average central density for globular clusters).

As a further implication of the present model, we stress that – at variance with the case of globular clusters – the mass spectrum of the dark clusters should be smooth, since the monotonic decrease of the PGC cloud temperature fails to single out any particular mass scale. As it will be shown in Sect. 3, dark clusters in the mass range  $3 \times 10^2 M_{\odot} \lesssim M_{DC} \lesssim 10^6 M_{\odot}$  should survive all disruptive effects, and so we shall restrict our attention to such a mass range throughout.

As far as dark clusters are concerned, we have seen that the brown dwarf mass is expected to lie in the range  $10^{-2} - 10^{-1} M_{\odot}$ . For definiteness (and with an eye to microlensing results), we imagine that all individual brown dwarfs have the same mass  $m \simeq 0.1 M_{\odot}$ . So, binary brown dwarfs are twice as heavy. As a consequence, the mass stratification instability (Spitzer [1969]) will drive them into the dark cluster cores, which then tend to be composed chiefly by binaries.

Furthermore, an average MACHO mass somewhat larger than  $\simeq 0.1 M_\odot$  can naturally be accounted for.

Finally, let us consider molecular clouds. Since they also originate from the above-mentioned fragmentation process, we suppose (for definiteness) that they lie in the mass range  $10^{-3} M_\odot \lesssim M_m \lesssim 10^{-1} M_\odot$ . Correspondingly, eq. (12) entails  $4.8 \times 10^{-5} \text{ pc} \lesssim r_m \lesssim 4.8 \times 10^{-3} \text{ pc}$  and  $2.7 \times 10^{10} \text{ cm}^{-3} \gtrsim n_m \gtrsim 2.7 \times 10^6 \text{ cm}^{-3}$ , respectively, where  $n_m$  denotes the number density in the clouds.

Before closing this Section, some comments are in order. There is little doubt that the foregoing considerations are qualitative in nature. Nevertheless, they provide nontrivial insights into several questions that arise in connection with the discovery of MACHOs. Specifically, a sharply peaked IMF in the range  $10^{-2} - 10^{-1} M_\odot$  comes out naturally without having to invoke any new physical process. This fact explains the observed absence of a substantial amount of main-sequence stars inside the dark clusters. Therefore, the observed absence of a large number of planet-like objects in the halo (Renault et al. [1997]) is automatically explained. Furthermore, we can understand why brown dwarfs clumped into dark clusters copiously form in the outer halo, but neither in the inner halo nor in the disk. Indeed, the different stellar content of these regions is here traced back to the different environments in which the *same* star formation mechanism operates. It goes without saying that various issues addressed above require further investigations.

### 3 Dynamical constraints on dark clusters

As we have seen, MACHOs are clumped into dark clusters when they form in the outer galactic halo. Still, the further fate of these clusters is quite unclear.

For, they might either evaporate or drift towards the galactic centre. In the latter case, encounters with globular clusters might have dramatic observational consequences and dynamical friction could drive too many MACHOs into the galactic bulge. So, even if dark clusters are unseen, nontrivial constraints on their characteristic parameters arise from the observed properties of our galaxy. Moreover, in order to play any rôle as a candidate for dark matter, MACHOs must have survived until the present in the outer part of the galactic halo. Finally, it is important to know whether MACHOs are still clumped into clusters today, especially because an improvement in the statistics of microlensing observations permits to test this possibility (Maoz [1994], Metcalf and Silk [1996]).

We remark that previous work on dynamical constraints on clusters of brown dwarfs (Carr and Lacey [1987], Carr [1994], Moore and Silk [1995], Gerhard and Silk [1996], Kerins [1996]) rests upon the hypothesis of an initial dark cluster distribution that extends inside the inner part of the Galaxy all the way down to the centre. Hence, a novel *ab initio* analysis is required within the present scenario.

We begin with the usual assumption that the halo dark matter density is modelled by an isothermal sphere <sup>12</sup> with density profile

$$\rho(R) = \rho_0 \frac{a^2 + R_0^2}{a^2 + R^2} \quad (14)$$

where  $a \simeq 5$  kpc is the halo core radius,  $R_0 \simeq 8.5$  kpc is our galactocentric distance and  $\rho_0 \simeq 6.5 \times 10^{-25}$  g cm<sup>-3</sup> denotes the local dark matter density corresponding to the one-dimensional velocity dispersion  $\sigma \simeq 155$  km s<sup>-1</sup> of

---

<sup>12</sup>As mentioned in Sect. 1, this model may not provide the best description of the Galaxy. However, it will still be used in the present Section since otherwise the ensuing discussion would become exceedingly complicated. Furthermore, it should be kept in mind that the various uncertainties affecting the dark cluster properties anyway make the following results reliable only as order-of-magnitude estimates.

the halo. Furthermore, we shall suppose for definiteness that the age of the Universe is  $t_0 \simeq 10^{10}$  yr. Our treatment of encounters rests upon the diffusion approximation and we will follow rather closely the analysis of Binney and Tremaine [1987].

### 3.1 Dynamical friction

Dark clusters are subject to dynamical friction as they orbit through the Galaxy, which makes them loose energy and therefore spiral in toward the galactic centre. Assuming (for illustrative purposes) that a dark cluster moves with velocity  $v$  on a circular orbit of radius  $R$ , the drag brought about by the background density  $\rho(R)$  is given by

$$F(R) = - 0.43 \frac{4\pi G^2 M_{DC}^2 \ln \Lambda}{v^2} \rho(R) \quad (15)$$

where  $\ln \Lambda$  is the usual Coulomb logarithm, whose value in the present case is

$$\ln \Lambda \simeq \ln \left( \frac{R_{typ} v^2}{GM_{DC}} \right) \simeq 24.3 - \ln(M_{DC}/M_\odot), \quad (16)$$

with  $R_{typ} \sim 20$  kpc,  $v \simeq \sqrt{2}\sigma$ . Using eq. (14), eq. (15) becomes

$$F(R) \simeq - 5.1 \times 10^{14} \ln \Lambda \left( \frac{M_{DC}}{M_\odot} \right)^2 \frac{1}{1 + R_5^2} \text{ g cm s}^{-2}, \quad (17)$$

where  $R_5$  is in units of 5 kpc. Accordingly, the equations of motion entail that a dark cluster originally at galactocentric distance  $R$  will be closer to the galactic centre today by the amount

$$\Delta R(R) \simeq 1.85 \times 10^{-8} \left( \frac{M_{DC}}{M_\odot} \right) \frac{24.3 - \ln(M_{DC}/M_\odot)}{R_5 + R_5^{-1}} \text{ kpc}. \quad (18)$$

Keeping in mind that in our model  $R > 10 - 20$  kpc and  $M_{DC} \lesssim 10^6 M_\odot$  (see later), we see that  $\Delta R \lesssim 5.8 \times 10^{-2}$  kpc. Therefore, *dark clusters are still confined in the outer galactic halo*. As a consequence, encounters between dark

and globular clusters as well as disk and bulge shocking of dark clusters are dynamically irrelevant, as long as they move on not too highly elongated orbits (in this way an effective circularization of the orbits is achieved).

### 3.2 Encounters between dark clusters

Encounters between dark clusters may – under the circumstances to be analyzed below – lead to their disruption. As an orientation, we notice that an estimate of the one-dimensional velocity dispersion  $\sigma_*$  of MACHOs and molecular clouds within a dark cluster is supplied by the virial theorem and reads

$$\sigma_* \simeq 6.9 \times 10^{-2} \left( \frac{M_{DC}}{M_\odot} \right)^{1/3} \text{ km s}^{-1}, \quad (19)$$

where eq. (13) has been used. Because in the present scenario  $M_{DC} \lesssim 10^6 M_\odot$  (see later), we get  $\sigma_* \lesssim 6.9 \text{ km s}^{-1}$ . Therefore, the one-dimensional velocity dispersion of dark clusters - which we naturally suppose to be just  $\sigma$  - is much larger than  $\sigma_*$ . Hence it makes sense to work within the impulse approximation, whose range of validity is established more precisely by the condition  $M_{DC} \ll 10^{10} M_\odot$ , which is evidently always met in our model.

In order to proceed further, we denote by  $\Delta E$  the change of the internal energy of a dark cluster in a single encounter. Then (following Binney and Tremaine [1987]) we find that encounters with impact parameter  $b$  in the range  $b_{\min} \leq b \leq b_{\max}$  increase the cluster's energy at the rate

$$\dot{E}(R) \simeq \sqrt{\pi} \frac{n_{DC}(R)}{\sigma^3} \int_0^\infty dv v^3 e^{-v^2/4\sigma^2} \int_{b_{\min}}^{b_{\max}} db b \Delta E \quad (20)$$

where  $v$  and  $n_{DC}(R)$  are the cluster velocity and number density (in the halo), respectively. We let  $\gamma$  stand for the fraction of halo dark matter in the form of dark clusters, so that we have  $n_{DC}(R) = \gamma\rho(R)/M_{DC}$ , with  $\rho(R)$  given by eq.

(14). Accordingly, eq. (20) becomes

$$\dot{E}(R) \simeq \frac{1}{2\sqrt{\pi}} \frac{\gamma}{\sigma GM_{DC}} \frac{1}{R^2 + a^2} \int_0^\infty dv v^3 e^{-v^2/4\sigma^2} \int_{b_{\min}}^{b_{\max}} db b \Delta E . \quad (21)$$

Now, a natural definition of the time required by encounters to dissolve a cluster is provided by  $t_d(R) = E_{\text{bind}}/\dot{E}(R)$ , where the binding energy  $E_{\text{bind}}$  is expressed in terms of the cluster properties as  $E_{\text{bind}} \simeq 0.2 GM_{DC}^2/r_{DC}$ .

### 3.2.1 Distant encounters

Let us consider first distant encounters. Correspondingly,  $\Delta E$  is to be evaluated in the tidal approximation (Spitzer [1987]) and reads presently

$$\Delta E \simeq \frac{4G^2 M_{DC}^3 r_{DC}^2}{3b^4 v^2} . \quad (22)$$

We insert this quantity into eq. (21), neglecting the term  $(b_{\min}/b_{\max})^2$  in the ensuing expression. Experience with a similar treatment for globular clusters suggests to choose  $b_{\min} \simeq r_{DC}$ . Correspondingly, we find

$$t_d(R) \simeq \frac{4.7 \times 10^{11}}{\gamma} \left( \frac{M_\odot}{M_{DC}} \right)^{1/3} (R_5^2 + 1) \text{ yr}, \quad (23)$$

where use of eq. (13) has been made. Assuming  $R > 10 - 20$  kpc and keeping in mind that  $\gamma \leq 1$  and  $M_{DC} \lesssim 10^6 M_\odot$  (see later), we get that for all the dark clusters in question  $t_d(R)$  exceeds the age of the Universe.

### 3.2.2 Close encounters

In order to deal with close encounters, dark clusters have to be regarded as extended objects. As in the case of globular clusters, this task is most simply accomplished by modelling the dark clusters by means of a Plummer potential with core radius  $\alpha$ . Correspondingly,  $\Delta E$  is found to be

$$\Delta E \simeq \frac{G^2 M_{DC}^3}{3\alpha^2 v^2} . \quad (24)$$

As before, we insert this quantity into eq. (21), assuming now  $b_{\min} \simeq 0$  and  $b_{\max} \simeq r_{DC}$ . In this way, we obtain

$$t_d(R) \simeq \frac{2.4 \times 10^{11}}{\gamma} \left( \frac{\alpha}{r_{DC}} \right)^2 \left( \frac{\text{pc}}{r_{DC}} \right) (R_5^2 + 1) \text{ yr} . \quad (25)$$

We proceed by recalling that

$$\alpha = \left( \frac{3M_{DC}}{4\pi\rho_*(0)} \right)^{1/3} , \quad (26)$$

where  $\rho_*(r)$  denotes the dark cluster mass density. Taking  $\rho_*(0) \simeq 10^4 M_\odot \text{ pc}^{-3}$  (as for globular clusters today) and using eq. (13), we can rewrite eq. (25) as

$$t_d(R) \simeq \frac{10^{11}}{\gamma} \left( \frac{M_\odot}{M_{DC}} \right)^{1/3} (R_5^2 + 1) \text{ yr} . \quad (27)$$

Assuming  $R > 10 - 20$  kpc and remembering that  $\gamma \leq 1$ , we are led to the conclusion that *dark clusters are not disrupted by close encounters* provided  $M_{DC} \lesssim 10^6 M_\odot$ .<sup>13</sup>

### 3.3 Evaporation

Various dynamical effects conspire to make dark clusters evaporate within a finite time. Relaxation via gravitational two-body encounters leads to the escape of MACHOs approaching the unbound tail of the cluster velocity distribution. Tidal truncation due to the galactic gravitational field enhances this process. A more substantial effect is caused by the gravothermal instability, when the inner part of the dark clusters contracts (core collapse) and the envelope expands.

Below, we shall address these issues separately. As is well known, a key-rôle in such an analysis is played by the relaxation time

$$t_{\text{relax}}(r) = 0.34 \frac{\sigma_*^3}{G^2 m \rho_*(r) \ln(0.4N)} \quad (28)$$

---

<sup>13</sup>It should hardly come as a surprise that close encounters yield a more stringent bound on  $M_{DC}$  than distant encounters.

where  $N$  is the number of MACHOs per cluster. As in the case of globular clusters,  $\rho_*(r)$  is expected to vary by various orders of magnitude in different regions of a single dark cluster – this dependence obviously shows up in  $t_{\text{relax}}(r)$ . Therefore, for reference purposes, it is often more convenient to characterize a dark cluster by a single value of the relaxation time. This goal is achieved by introducing the median relaxation time (Spitzer and Hart [1971])

$$t_{\text{rh}} = \frac{6.5 \times 10^8}{\ln(0.4N)} \left( \frac{M_{DC}}{10^5 M_\odot} \right)^{1/2} \left( \frac{M_\odot}{m} \right) \left( \frac{r_{DC}}{\text{pc}} \right)^{3/2} \text{ yr} . \quad (29)$$

Explicitly, using eq. (13) together with eq. (19) and  $m \simeq 0.1 M_\odot$ , eq. (28) takes the form <sup>14</sup>

$$t_{\text{relax}}(r) \simeq 5 \times 10^7 \left( \frac{M_{DC}}{M_\odot} \right) \left( \frac{M_\odot \text{ pc}^{-3}}{\rho_*(r)} \right) \frac{1}{1.4 + \ln(M_{DC}/M_\odot)} \text{ yr} . \quad (30)$$

In the same fashion, eq. (29) becomes

$$t_{\text{rh}} \simeq 8 \times 10^5 \left( \frac{M_{DC}}{M_\odot} \right) \frac{1}{1.4 + \ln(M_{DC}/M_\odot)} \text{ yr} . \quad (31)$$

### 3.3.1 Spontaneous evaporation

As is well known, any stellar association evaporates spontaneously <sup>15</sup> within a finite time owing to relaxation via gravitational two-body encounters. Specifically, a single close encounter between two MACHOs can leave one of them with a speed larger than the local escape velocity. So, the MACHO under consideration gets ejected from the dark cluster. We find for the ejection time (Hénon [1969]),

$$t_{\text{ej}} \simeq 1.1 \times 10^3 \ln(0.4N) t_{\text{rh}} \simeq 9 \times 10^8 \left( \frac{M_{DC}}{M_\odot} \right) \text{ yr} . \quad (32)$$

---

<sup>14</sup>For simplicity, we neglect here the fact that binaries have a mass larger than individual brown dwarfs. Furthermore, given the logarithmic  $N$ -dependence, we can safely take  $N \sim M_{DC}/m \sim 10 (M_{DC}/M_\odot)$ .

<sup>15</sup>We like to call in this way the evaporation process which is neither induced by external perturbations nor specific of the gravitational interactions.



Alternatively, several more distant weaker encounters can gradually increase the energy of a given MACHO, until a further weak encounter is sufficient to make it escape from the cluster. In this case, the evaporation time turns out to be (Spitzer and Thuan [1972])

$$t_{\text{evap}} \simeq 300 t_{\text{rh}} \simeq 2.4 \times 10^8 \left( \frac{M_{DC}}{M_{\odot}} \right) \frac{1}{1.4 + \ln(M_{DC}/M_{\odot})} \text{ yr.} \quad (33)$$

Since  $t_{\text{ej}}$  is anyway longer than  $t_{\text{evap}}$ , we shall focus our attention on the latter quantity. Hence, by demanding that  $t_{\text{evap}}$  should exceed the age of the Universe we conclude that *dark clusters with  $M_{DC} \gtrsim 3 \times 10^2 M_{\odot}$  are not yet evaporated.*

### 3.3.2 Tidal Perturbations

Dark clusters – just like globular clusters – are tidally disrupted by the galactic gravitational field unless  $r_{DC}$  is smaller than their tidal radius. So, the survival condition reads

$$r_{DC} < \left( \frac{M_{DC}}{3M_G(R)} \right)^{1/3} R, \quad (34)$$

where  $R$  should be understood here as the perigalactic distance of the dark cluster and  $M_G(R)$  denotes the Galaxy mass inside  $R$ . From eq. (14) we obtain

$$M_G(R) \simeq 5.5 \times 10^{10} R_5 (1 - R_5^{-1} \arctan R_5) M_{\odot}, \quad (35)$$

and - on account of eq. (13) - eq. (34) becomes

$$R_5 [1 - R_5^{-1} \arctan R_5]^{-1/2} > 0.047, \quad (36)$$

which is always satisfied for  $R > 10 - 20$  kpc. Thus, the dark clusters under consideration are not tidally disrupted by the galactic gravitational field.

### 3.3.3 Core collapse

An important rôle in the considerations to follow is played by core collapse. It is by now well-established that the initial stage of this process is triggered by evaporation, which leads to the shrinking of the core as a consequence of energy conservation. Numerical Fokker-Planck studies of the early phase of core collapse have shown that the dynamics of the cluster is correctly described by a sequence of King models (Cohn [1980]). However, once the cluster density reaches a certain critical value, core collapse gets dramatically accelerated by the gravothermal instability (Antonov [1962], Lynden-Bell and Wood [1968]). Indeed, the negative specific heat of the core implies that the internal velocity dispersion  $\sigma_*$  increases – thereby enhancing evaporation – as the average kinetic energy decreases by evaporation itself. Moreover, the unbalanced gravitational energy makes the core contract, and so its density rises by several orders of magnitude in a runaway manner. Numerical simulations show that the central velocity dispersion and the number of stars in the core  $N_*$  scale as

$$\sigma_* \sim \rho_*(0)^{0.05}, \quad (37)$$

$$N_* \sim \rho_*(0)^{-0.36}, \quad (38)$$

respectively (Binney and Tremaine [1987]). Incidentally, the somewhat surprising slow rise of  $\sigma_*$  in eq. (37) is due to the large mass-loss from the core, as it follows from eq. (38).

When does the gravothermal instability show up? Unfortunately, a clear-cut answer does not exist, since the corresponding time  $t_{GI}$  depends on how clusters are modelled as well as on their concentration (Quinlan [1996]). Manifestly, the lack of observational data about dark clusters makes a precise determination of

$t_{GI}$  impossible. So, the best we can do is to suppose that dark clusters behave just like globular clusters as far as core collapse is concerned. In this way, we are lead to the order-of-magnitude estimate (Binney and Tremaine [1987]) (more about this, later)

$$t_{GI} \simeq 3 t_{rh} \simeq 2.4 \times 10^6 \left( \frac{M_{DC}}{M_{\odot}} \right) \frac{1}{1.4 + \ln(M_{DC}/M_{\odot})} \text{ yr} . \quad (39)$$

Comparing now  $t_{GI}$  with the age of the Universe, we conclude that *the dark clusters with  $M_{DC} \lesssim 5 \times 10^4 M_{\odot}$  are expected to have started core collapse.*

As we said, the central density grows dramatically during the second stage of core collapse, and so the central relaxation time gets shorter and shorter. Detailed studies of the gravothermal instability have shown that – if nothing opposes to collapse – the time needed to complete core collapse  $t_{\text{coll}}$  starting from an arbitrary time  $t$  goes like  $t_{\text{relax}}(0)$ , with the latter quantity computed for the particular value taken by  $\rho_*(0)$  at  $t$ . More specifically, computer simulations of globular cluster dynamics entail  $t_{\text{coll}} \simeq 330 t_{\text{relax}}(0)$  (Cohn [1980]).

Because of the huge increase in the central density, close two-body encounters lead to the formation of bound binary systems by converting enough kinetic energy into internal energy (tidal capture). As we will see in Section 4, binary brown dwarfs are produced in this way in the dark cluster cores during the early phase of core collapse. These binaries - which will be referred to as *tidally-captured* binaries and happen to be very hard - play a crucial rôle in this context, since they ultimately stop and reverse the collapse. Schematically, the argument goes as follows. Owing to the fact that hard binaries necessarily get harder in collisions with individual stars (Heggie [1975]), the internal binding energy released by a binary is transformed into kinetic energy of both the star and the binary. Actually, the exchanged energy is so large that they both leave

the cluster. However – at variance with evaporation – the kinetic energy (per unit mass) of the cluster is now unaffected, whereas mass ejection obviously increases the potential energy. That is, the binding energy given up by the binaries ultimately becomes gravitational energy of the core. As a result of the unbalanced kinetic energy, the core starts expanding. Moreover, because of the negative specific heat the increased potential energy makes  $\sigma_*$  decrease, thereby slowing down mass ejection. In this manner, core collapse gets halted and reversed (Spitzer [1987]).

As a matter of fact, the presence of binaries in appreciable amount can also modify to some extent the standard scenario of core collapse as outlined above. Indeed, numerical Fokker-Planck simulations have shown that in this case the collapse is also driven by the mass stratification instability. As a consequence, the collapse proceeds faster and starts before than in the few-binary case (the latter point makes eq. (39) more plausible than it might appear at first sight). This phenomenon is found to occur both for tidally-captured binaries (Statler, Ostriker and Cohn [1987]) and for primordial binaries (Spitzer and Mathieu [1980]).

### 3.4 Discussion

What the above analysis shows is that dark clusters within the mass range  $3 \times 10^2 M_\odot \lesssim M_{DC} \lesssim 10^6 M_\odot$  should have survived all disruptive effects arising from gravitational perturbations and are nowadays expected to populate the outer part of the galactic halo. In addition, the clusters with  $3 \times 10^2 M_\odot \lesssim M_{DC} \lesssim 5 \times 10^4 M_\odot$  should undergo core collapse. Unfortunately, it is practically impossible to predict the further fate of those dark clusters which are in the post-collapse

phase today. *A priori* it seems natural to imagine that bounce and subsequent reexpansion should follow core collapse (Cohn and Hut [1984], Heggie and Ramamani [1989]). And perhaps also a whole series of core contractions and expansions can take place, giving rise to the so-called gravothermal oscillations (Bettwieser and Sugimoto [1984]). However, this conclusion crucially depends on the unknown model which correctly describes dark clusters. For instance, in the case of tidally-truncated models the cluster gets completely destroyed within a finite time (Stodolkiewicz [1985], Ostriker, Statler and Lee [1985]). Moreover, what certainly happens in either case is that the number of MACHOs in the core monotonically decreases with time. So, an unclustered MACHO population is expected to coexist with dark clusters in the outer galactic halo (unless all dark clusters have  $M_{DC} \gtrsim 5 \times 10^4 M_{\odot}$ ) – detection of unclustered MACHOs would therefore not rule out the present scenario.

## 4 MACHOs as binary brown dwarfs

As already pointed out, it seems natural to suppose that a fraction of primordial binary brown dwarfs – possibly as large as 50% in mass – should form along with individual brown dwarfs as a result of the fragmentation process of the PGC clouds. Subsequently, because of the mass stratification instability primordial binaries will concentrate inside the dark cluster cores, which are therefore expected to be chiefly composed by binaries and molecular clouds. In addition – as far as dark clusters with  $M_{DC} \lesssim 5 \times 10^4 M_{\odot}$  are concerned – a population of tidally-captured binary brown dwarfs ought to form in the dark cluster cores owing to the increased central density caused by core collapse. Thus, a large fraction of binaries should be present inside the dark cluster cores at a late

stage of their evolution. Below, we will try to make the discussion of this issue as much quantitative as possible.

#### 4.1 Survival and hardness of binary brown dwarfs

The first question that has to be addressed is whether a binary brown dwarf – produced by whatever mechanism long ago – survives up until the present. To this end, we recall that a binary system is *hard* when its binding energy exceeds the kinetic energy of field stars (otherwise it is *soft*). In the present case, binary brown dwarfs happen to be hard when their orbital radius  $a$  obeys the following constraint

$$a \lesssim 1.4 \times 10^{12} \left( \frac{M_{\odot}}{M_{DC}} \right)^{2/3} \text{ km} . \quad (40)$$

As is well known, soft binaries always get softer whereas hard binaries always get harder because of encounters with individual stars (Heggie [1975]). So – were individual-binary encounters the only relevant process – we would conclude that hard binary brown dwarfs should indeed survive. However, also binary-binary encounters play an important rôle in the dark cluster cores, where binaries are expected to be far more abundant than individual brown dwarfs. Now, in the latter process one of the two binaries gets often disrupted (this cannot happen for both binaries – given that they are hard – while fly bys are rather infrequent), thereby leading to the depletion of the binary population. We will address this effect in Sect. 4.3, where we shall find that for realistic values of the dark cluster parameters the binary break up does not take place.

#### 4.2 Tidally-captured binary brown dwarfs

As far as globular clusters are concerned, it is nowadays well known that the most efficient mechanism for late binary formation is dissipative tidal capture in

the core (Fabian, Pringle and Rees [1975], Press and Teukolsky [1977], Lee and Ostriker [1986]). Hence, we expect a similar situation to occur for dark clusters as well.

Let us now analyze this phenomenon in a quantitative fashion. As a first step, we observe that the radius  $r_*$  of a brown dwarf of mass  $\simeq 0.1M_\odot$  is  $r_* \simeq 0.7 \times 10^5$  km (Saumon et al. [1996]). Furthermore, the Safronov number (Binney and Tremaine [1987]) is

$$\Theta = \frac{Gm}{2\sigma_*^2 r_*} \simeq 2 \times 10^7 \left( \frac{M_\odot}{M_{DC}} \right)^{2/3}, \quad (41)$$

which turns out to be anyway much larger than one. Within this approximation, the time for brown dwarf tidal capture can be written as (Lee and Ostriker [1986])

$$t_{\text{tid}} \simeq 10^{12} \left( \frac{10^5 \text{ pc}^{-3}}{n_{IBD}(0)} \right) \left( \frac{\sigma_*}{100 \text{ km s}^{-1}} \right)^{1.2} \left( \frac{R_\odot}{r_*} \right)^{0.9} \left( \frac{M_\odot}{m} \right)^{1.1} \text{ yr}, \quad (42)$$

where  $n_{IBD}(0)$  is the number density of individual brown dwarfs in the core <sup>16</sup>. Obviously, we have  $n_{IBD}(0) \simeq f_{IBD} \rho_*(0)/m$ , with  $f_{IBD}$  denoting the mass fraction of individual brown dwarfs in the core. From eq. (37) we see that  $\sigma_*$  increases very slightly, and so core collapse effects on  $\sigma_*$  can safely be neglected. Accordingly, we can rewrite eq. (42) as

$$t_{\text{tid}} \simeq \frac{1.6 \times 10^{14}}{f_{IBD}} \left( \frac{M_\odot \text{ pc}^{-3}}{\rho_*(0)} \right) \left( \frac{M_{DC}}{M_\odot} \right)^{0.4} \text{ yr} \quad (43)$$

where eq. (19) has been used. Comparing now  $t_{\text{tid}}$  with the age of the Universe, we get that practically all individual brown dwarfs in the core are tidally

<sup>16</sup>Although eq. (42) has been derived for main-sequence stars, it looks plausible that it applies also to brown dwarfs, since it is not very sensitive to the particular stellar model (Lee and Ostriker [1986]).

captured into binaries provided <sup>17</sup>

$$\rho_*(0) > \frac{3.2 \times 10^4}{f_{IBD}} \left( \frac{M_{DC}}{M_\odot} \right)^{0.4} M_\odot \text{ pc}^{-3} . \quad (44)$$

According to the above assumptions, we expect  $\rho_*(0) \simeq 10^4 M_\odot \text{ pc}^{-3}$  just before core collapse. Therefore, we see that tidal capture requires an increase of  $\rho_*(0)$  by a factor in the range  $31/f_{IBD} - 242/f_{IBD}$ , corresponding to  $M_{DC}$  in the range  $3 \times 10^2 M_\odot - 5 \times 10^4 M_\odot$ . Thus, the formation of tidally-captured binaries would occur during the early phase of core collapse (the same conclusion was reached in a different way by Statler, Ostriker and Cohn [1987] for globular clusters). However, this conclusion depends on the fractional (mass) abundance  $f_{PB}$  of primordial binaries in the core, since  $f_{IBD}$  necessarily gets small for large  $f_{PB}$ .

Next, we compute the (average) orbital radius of tidally-captured binary brown dwarfs following the procedure outlined by Statler, Ostriker and Cohn [1987]. Correspondingly, we find  $a \simeq 2.5 \times 10^5 \text{ km}$  (this value is practically independent of  $M_{DC}$ ). As a consequence, we see that they are so hard that condition (40) is always abundantly met.

Let us finally try to estimate the fractional abundance of tidally-captured binary brown dwarfs in the dark cluster cores soon after their formation, namely when inequality (44) just starts to be satisfied (their total number at this stage will be denoted by  $N_{TCB}$ ). Thanks to eq. (38) we easily get

$$N_{TCB} \simeq 3.3 f_{IBD}^{1.36} \left( \frac{M_{DC}}{M_\odot} \right)^{0.86} \left( \frac{M_c}{M_\odot} \right) , \quad (45)$$

---

<sup>17</sup>More precisely, we are demanding that the rate for tidal capture times the age of the Universe should exceed one. Notice that the former quantity is one-half of  $t_{\text{tid}}^{-1}$ , and so we require that  $2t_{\text{tid}}$  should be smaller than  $10^{10} \text{ yr}$  (we are actually following the same procedure used by Press and Teukolsky [1977]).



where  $M_c$  denotes the core mass just before core collapse (corresponding to  $\rho_*(0) \simeq 10^4 M_\odot \text{pc}^{-3}$ ). Denoting further by  $N_{IBD}^{\text{tot}}$  the total number of individual brown dwarfs in a dark cluster before core collapse, we find

$$\frac{N_{TCB}}{N_{IBD}^{\text{tot}}} \simeq 0.33 f_{IBD}^{0.36} \left( \frac{M_\odot}{M_{DC}} \right)^{0.14} \left( \frac{M_c}{M_{DC}} \right). \quad (46)$$

Realistically, even in the extreme case of a fully baryonic halo we expect  $f_{IBD} \lesssim 0.3$  (of course, a large  $f_{PB}$  would imply a  $f_{IBD}$  considerably smaller than that). Moreover,  $M_c/M_{DC}$  sensitively depends on how the core is defined, but the analogy with globular clusters entails that it should anyway be less than 20%. Accordingly, we conclude that the fractional abundance of tidally-captured binary brown dwarfs should not exceed 1% (again in remarkable agreement with the result of Statler, Ostriker and Cohn [1987] for globular clusters), and so they are irrelevant from the observational point of view.

### 4.3 Primordial binary brown dwarfs

Primordial binaries are a very different story. For, not only are they expected to be much more abundant than tidally-captured binaries, but in addition they are presumably much less hard, since all values for their orbital radius consistent with condition (40) are in principle to be contemplated. So, hardening effects ought to play a crucial rôle for primordial binaries (as it can be guessed on intuitive grounds, effects of this kind turn out to be totally negligible for tidally-captured binaries – this will be demonstrated later on).

#### 4.3.1 Collisional hardening

Let us begin by considering collisional hardening, namely the process whereby hard binaries get harder in encounters with individual brown dwarfs. We recall

that the associated average hardening rate (Spitzer & Mathieu 1980) reads presently

$$\dot{E} \simeq - 2.8 \frac{G^2 m^3 n_{IBD}(0)}{\sigma_*} . \quad (47)$$

On account of the definition of  $n_{IBD}(0)$  and of eq. (19), eq. (47) becomes

$$\dot{E} \simeq - 1.7 \times 10^{32} f_{IBD} \left( \frac{M_\odot}{M_{DC}} \right)^{1/3} \left( \frac{\rho_*(0)}{M_\odot \text{ pc}^{-3}} \right) \text{ erg yr}^{-1} . \quad (48)$$

Observe that a characteristic feature of collisional hardening is that  $\dot{E}$  is independent of hardness, and so it is time-independent.

As is well known, the internal energy of a binary is  $E = -Gm^2/2a$ , which yields

$$\dot{E} = \frac{Gm^2}{2a^2} \dot{a} . \quad (49)$$

Hence, by combining eqs. (48) and (49) together and integrating the ensuing expression we get

$$\frac{\text{km}}{a_2} \simeq \frac{\text{km}}{a_1} + 1.3 \times 10^{-20} f_{IBD} \left( \frac{M_\odot}{M_{DC}} \right)^{1/3} \left( \frac{\rho_*(0)}{M_\odot \text{ pc}^{-3}} \right) \left( \frac{t_{21}}{\text{yr}} \right) , \quad (50)$$

where  $a_1$  stands for the initial orbital radius, whereas  $a_2$  denotes the orbital radius after a time  $t_{21}$ .

Assuming momentarily that no other hardening mechanism is operative and taking  $t_{21}$  equal to the age of the Universe, we find that the present orbital radius of a binary brown dwarf is given by

$$\frac{\text{km}}{a_2} \simeq \frac{\text{km}}{a_1} + 1.3 \times 10^{-10} f_{IBD} \left( \frac{M_\odot}{M_{DC}} \right)^{1/3} \left( \frac{\rho_*(0)}{M_\odot \text{ pc}^{-3}} \right) . \quad (51)$$

Of course, collisional hardening works to the extent that  $a_2$  becomes considerably smaller than  $a_1$ . Correspondingly, we see from eq. (51) that this is indeed the case provided

$$a_1 \gtrsim 8 \times 10^9 f_{IBD}^{-1} \left( \frac{M_{DC}}{M_\odot} \right)^{1/3} \left( \frac{M_\odot \text{ pc}^{-3}}{\rho_*(0)} \right) \text{ km} . \quad (52)$$

Thanks to eq. (51), eq. (52) yields in turn

$$a_2 \simeq 8 \times 10^9 f_{IBD}^{-1} \left( \frac{M_{DC}}{M_\odot} \right)^{1/3} \left( \frac{M_\odot \text{ pc}^{-3}}{\rho_*(0)} \right) \text{ km} . \quad (53)$$

Physically, the emerging picture is as follows. Only those binaries whose initial orbital radius obeys condition (52) undergo collisional hardening, and their present orbital radius turns out to be almost *independent* of the initial value. We can make the present discussion somewhat more specific by noticing that our assumptions strongly suggest  $\rho_*(0) \lesssim 10^4 M_\odot \text{ pc}^{-3}$ , in which case both eq. (52) and eq. (53) acquire the form

$$a_{1,2} \gtrsim 8 \times 10^5 f_{IBD}^{-1} \left( \frac{M_{DC}}{M_\odot} \right)^{1/3} \text{ km} . \quad (54)$$

Evidently, very hard primordial binaries – which fail to meet condition (54) – do not suffer collisional hardening, and the same is true for tidally-captured binaries.

### 4.3.2 Frictional hardening

As we are going to show, the presence of molecular clouds in the dark cluster cores – which is indeed the most characteristic feature of the model in question – provides a novel hardening mechanism for binary brown dwarfs. Basically, this is brought about by dynamical friction on molecular clouds.

It is not difficult to extend the standard treatment of dynamical friction (Binney & Tremaine [1987]) to the relative motion of the brown dwarfs in a binary system which moves inside a molecular cloud. For simplicity, we assume that molecular clouds have a constant density profile  $\rho_m$ . In the case of a circular orbit <sup>18</sup>, the equations of motion imply that the time  $t_{21}^{(0)}$  needed to reduce the

<sup>18</sup>Indeed, the circularization of the orbit is achieved by tidal effects after a few periastron passages (Zahn 1987).

orbital radius  $a$  of a binary which moves *all the time* inside molecular clouds from  $a_1$  down to  $a_2$  is

$$t_{21}^{(0)} \simeq 0.17 \left(\frac{m}{G}\right)^{1/2} \frac{1}{\rho_m \ln \Lambda} (a_2^{-3/2} - a_1^{-3/2}), \quad (55)$$

where the Coulomb logarithm reads

$$\ln \Lambda \simeq \ln(r_m v_c^2 / Gm) \simeq \ln(r_m / a_1), \quad (56)$$

with  $v_c$  denoting the circular velocity (approximately given by Kepler's third law). Manifestly, the diffusion approximation – upon which the present treatment is based – requires that the orbital radius of a binary should always be smaller than the median radius of a cloud. As we are concerned henceforth with hard binaries,  $a_1$  has to obey condition (40). On the other hand,  $a_1$  is the larger value for the orbital radius in eq. (55). So, we shall take for definiteness – in the Coulomb logarithm only –  $a_1 \simeq 1.4 \times 10^{12} (M_\odot / M_{DC})^{2/3}$  km. In addition, from eq. (12) we have

$$\rho_m \simeq 2.5 \left(\frac{\text{pc}}{r_m}\right)^2 M_\odot \text{pc}^{-3}. \quad (57)$$

Hence, putting everything together we obtain

$$\left(\frac{\text{km}}{a_2}\right)^{3/2} \simeq \left(\frac{\text{km}}{a_1}\right)^{3/2} + 2 \times 10^{-26} \Xi^{-1} \left(\frac{\text{pc}}{r_m}\right)^2 \left(\frac{t_{21}^{(0)}}{\text{yr}}\right), \quad (58)$$

having set

$$\Xi \equiv [3 + \ln(r_m / \text{pc}) + 0.7 \ln(M_{DC} / M_\odot)]^{-1}. \quad (59)$$

Specifically, the diffusion approximation demands  $\Xi > 0$ , which yields in turn

$$r_m > 5 \times 10^{-2} \left(\frac{M_\odot}{M_{DC}}\right)^{0.7} \text{pc}. \quad (60)$$

Observe that for  $M_{DC} \lesssim 2.1 \times 10^4 M_\odot$  this constraint restricts the range of allowed values of  $r_m$  as stated in Sect. 2.2.

Were the dark clusters completely filled by clouds, eq. (58) would be the final result. However, the distribution of the clouds is lumpy. So, if we want to know the orbital radius  $a_2$  after a time  $t_{21}$  we have to proceed as follows. First, we should compute the fraction  $t_{21}^{(0)}$  of the time interval in question  $t_{21}$  spent by a binary inside the clouds. Next, we have to re-express  $t_{21}^{(0)}$  in eq. (58) in terms of  $t_{21}$ . This goal will be achieved by the procedure outlined below.

Keeping in mind that both the clouds and the binaries have average velocity  $v \simeq \sqrt{3}\sigma_*$  (for simplicity, we neglect the equipartition of kinetic energy of the binaries) it follows that the time needed by a binary to cross a single cloud is

$$t_m \simeq \frac{r_m}{\sqrt{2} v} \simeq 5.6 \times 10^6 \left( \frac{r_m}{\text{pc}} \right) \left( \frac{M_\odot}{M_{DC}} \right)^{1/3} \text{ yr} . \quad (61)$$

As an indication, we notice that for  $r_m \simeq 10^{-3}$  pc ( $M_m \simeq 2 \times 10^{-2} M_\odot$ ) and  $M_{DC} \simeq 10^5 M_\odot$  we find  $t_m \simeq 1.2 \times 10^2$  yr. Therefore, frictional hardening involves many clouds. Specifically, during the time  $t_{21}$  the number of clouds crossed by a binary is evidently

$$N_m \simeq \frac{t_{21}^{(0)}}{t_m} \simeq 1.8 \times 10^{-7} \left( \frac{\text{pc}}{r_m} \right) \left( \frac{M_{DC}}{M_\odot} \right)^{1/3} \left( \frac{t_{21}^{(0)}}{\text{yr}} \right) . \quad (62)$$

Let us now ask how many crossings of the core are necessary for a binary to traverse  $N_m$  clouds. To this end, we proceed to estimate the number of clouds  $N_c$  encountered during *one* crossing of the core. Describing the dark clusters by a King model, we can identify the core radius with the King radius. Evidently, the cross-section for binary-cloud encounters is  $\pi r_m^2$  and so we have

$$N_c \simeq \left( \frac{9\sigma_*^2}{4\pi G\rho_*(0)} \right)^{1/2} n_{CL}(0) \pi r_m^2 , \quad (63)$$

with  $n_{CL}(0)$  denoting the cloud number density in the core. Thanks to eq. (12),

we can write

$$n_{CL}(0) \simeq f_{CL} \frac{\rho_*(0)}{M_m} \simeq 4.8 \times 10^{-2} f_{CL} \left( \frac{\text{pc}}{r_m} \right) \left( \frac{\rho_*(0)}{M_\odot \text{pc}^{-3}} \right) \text{pc}^{-3}, \quad (64)$$

where  $f_{CL}$  denotes the fraction of core dark matter in the form of molecular clouds. Correspondingly, eq. (63) becomes

$$N_c \simeq 0.13 \times f_{CL} \left( \frac{\rho_*(0)}{M_\odot \text{pc}^{-3}} \right)^{1/2} \left( \frac{M_{DC}}{M_\odot} \right)^{1/3} \left( \frac{r_m}{\text{pc}} \right), \quad (65)$$

on account of eq. (19). So, the total number of core crossings  $N_{cc}$  that a binary has to make in order to traverse  $N_m$  clouds is

$$N_{cc} \simeq \frac{N_m}{N_c} \simeq 1.4 \times 10^{-6} f_{CL}^{-1} \left( \frac{M_\odot \text{pc}^{-3}}{\rho_*(0)} \right)^{1/2} \left( \frac{\text{pc}}{r_m} \right)^2 \left( \frac{t_{21}^{(0)}}{\text{yr}} \right). \quad (66)$$

Because the core crossing time is

$$t_{cc} \simeq \left( \frac{9\sigma_*^2}{4\pi G \rho_*(0)} \right)^{1/2} \frac{1}{v} \simeq 7 \times 10^6 \left( \frac{M_\odot \text{pc}^{-3}}{\rho_*(0)} \right)^{1/2} \text{yr}, \quad (67)$$

it follows that the process under consideration takes a total time  $N_{cc} t_{cc}$ . However, this time is by definition just  $t_{21}$ . So, we get

$$t_{21} \simeq N_{cc} t_{cc} \simeq 9.8 f_{CL}^{-1} \left( \frac{M_\odot \text{pc}^{-3}}{\rho_*(0)} \right) \left( \frac{\text{pc}}{r_m} \right)^2 t_{21}^{(0)}, \quad (68)$$

which is the desired relationship between  $t_{21}$  and  $t_{21}^{(0)}$ . We are now in position to re-express eq. (58) in terms of  $t_{21}$ . Accordingly, we get

$$\left( \frac{\text{km}}{a_2} \right)^{3/2} \simeq \left( \frac{\text{km}}{a_1} \right)^{3/2} + 2.1 \times 10^{-27} f_{CL} \Xi^{-1} \left( \frac{\rho_*(0)}{M_\odot \text{pc}^{-3}} \right) \left( \frac{t_{21}}{\text{yr}} \right). \quad (69)$$

In order to quantify the effect of frictional hardening, we may proceed much in the same way as in the case of collisional hardening, neglecting however the latter effect for the moment. Specifically, taking  $t_{21}$  in eq. (69) equal to the age

of the Universe, we find that the present orbital radius of a binary brown dwarf is given by

$$\left(\frac{\text{km}}{a_2}\right)^{3/2} \simeq \left(\frac{\text{km}}{a_1}\right)^{3/2} + 2.1 \times 10^{-17} f_{CL} \Xi^{-1} \left(\frac{\rho_*(0)}{M_\odot \text{ pc}^{-3}}\right). \quad (70)$$

Manifestly, frictional hardening is operative to the extent that  $a_2$  becomes considerably smaller than  $a_1$ . Accordingly, from eq. (70) we see that this is indeed the case provided

$$a_1 \gtrsim 1.3 \times 10^{11} f_{CL}^{-2/3} \Xi^{2/3} \left(\frac{M_\odot \text{ pc}^{-3}}{\rho_*(0)}\right)^{2/3} \text{ km}. \quad (71)$$

Owing to eq. (71), eq. (70) entails in turn

$$a_2 \simeq 1.3 \times 10^{11} f_{CL}^{-2/3} \Xi^{2/3} \left(\frac{M_\odot \text{ pc}^{-3}}{\rho_*(0)}\right)^{2/3} \text{ km}. \quad (72)$$

Physically, only those binaries whose initial orbital radius satisfies condition (71) are affected by frictional hardening, and their present orbital radius turns out to be almost *independent* of the initial value. We can make the present discussion somewhat more specific by noticing that our assumptions strongly suggest  $\rho_*(0) \lesssim 10^4 M_\odot \text{ pc}^{-3}$ , in which case both eq. (71) and eq. (72) acquire the form

$$a_{1,2} \gtrsim 2.8 \times 10^8 f_{CL}^{-2/3} \Xi^{2/3} \text{ km}. \quad (73)$$

Evidently, very hard primordial binaries – which violate condition (73) – do not suffer frictional hardening, and the same is true for tidally-captured binaries.

### 4.3.3 Present orbital radius of primordial binaries

Which of the two hardening mechanisms under consideration is more effective? A straightforward implication of eqs. (53) and (72) is that frictional hardening

is more efficient than collisional hardening whenever it so happens that

$$f_{IBD} < 6.3 \times 10^{-2} f_{CL}^{2/3} \Xi^{-2/3} \left( \frac{M_{DC}}{M_{\odot}} \right)^{1/3} \left( \frac{M_{\odot} \text{pc}^{-3}}{\rho_*(0)} \right)^{1/3}. \quad (74)$$

Unfortunately, the occurrence of various dark cluster parameters in condition (74) does not permit a sharp conclusion to be drawn, but in the illustrative case  $M_{DC} \simeq 10^5 M_{\odot}$ ,  $r_m \simeq 10^{-3}$  pc,  $f_{CL} \simeq 0.5$  and  $\rho_*(0) \simeq 10^3 M_{\odot} \text{pc}^{-3}$  we get  $f_{IBD} < 0.5$ . As we expect in the cores  $f_{IBD} \ll f_{PB}$  and  $f_{CL} \simeq f_{PB}$ , we see that *frictional hardening plays the dominant rôle*. Moreover, from eqs. (53) and (72) it also follows that the effectiveness of collisional hardening decreases for smaller values of  $f_{IBD}$ . Finally, the fairly slow dependence of condition (74) on  $M_{DC}$  and  $\rho_*(0)$  makes our conclusion rather robust.

Having shown that collisional hardening can effectively be disregarded, we get that the present orbital radius of primordial binary brown dwarfs is actually given by eq. (72), as long as condition (71) is met. Taking again the above particular case as an illustration, we find  $a_2 \simeq 7 \times 10^8$  km, which is of the same order as the Einstein radius for microlensing towards the LMC (Gaudi and Gould [1997]). Therefore, we argue that not too hard primordial binaries can be resolved in future microlensing experiments with a more accurate photometric observation, the signature being small deviations from standard microlensing light curves (Dominik [1996]).

#### 4.3.4 Gravitational encounters

We are now in position to take up the question concerning the survival of binary brown dwarfs against gravitational encounters. As already pointed out, individual-binary encounters are harmless in this respect – since hard binaries are considered throughout – and so we shall restrict our attention to binary-



binary encounters.

As a first step, we recall that their average rate  $\Gamma$  (Spitzer & Mathieu 1980) can presently be written as

$$\Gamma \simeq \alpha \frac{Gma}{\sigma_*}, \quad (75)$$

with  $\alpha \simeq 13$ . Correspondingly, on account of eq. (19) the reaction time in the dark cluster cores turns out to be

$$t_{\text{react}} \simeq 10^{19} \beta \left( \frac{M_\odot \text{ pc}^{-3}}{\rho_*(0)} \right) \left( \frac{M_{DC}}{M_\odot} \right)^{1/3} \left( \frac{\text{km}}{a} \right) \text{ yr}, \quad (76)$$

with  $\beta \simeq 6.7/f_{PB}$ .

Now, if no hardening were to occur – which means that the orbital radius  $a$  would stay constant – the binary survival condition would simply follow by demanding that  $t_{\text{react}}$  should exceed the age of the Universe. However, hardening makes  $a$  decrease, and so  $t_{\text{react}}$  increases with time. This effect can be taken into account by considering the average value  $\langle t_{\text{react}} \rangle$  of the reaction time over the time interval in question (to be denoted by  $T$ ), namely

$$\langle t_{\text{react}} \rangle \equiv \frac{1}{T} \int_0^T dt t_{\text{react}}. \quad (77)$$

In order to compute  $\langle t_{\text{react}} \rangle$ , the temporal dependence  $a(t)$  of the binary orbital radius is needed. Because frictional hardening plays the major rôle, the latter quantity is evidently supplied by eq. (69). Setting for notational convenience  $t \equiv t_{21}$  and  $a(t) \equiv a_2$ , eq. (69) yields

$$a(t) \simeq \left[ \left( \frac{\text{km}}{a_1} \right)^{3/2} + 2.1 \times 10^{-27} \Xi^{-1} f_{CL} \left( \frac{\rho_*(0)}{M_\odot \text{ pc}^{-3}} \right) \left( \frac{t}{\text{yr}} \right) \right]^{-2/3} \text{ km}. \quad (78)$$

Combining eqs. (76) and (78) together and inserting the ensuing expression into eq. (77), we get

$$\langle t_{\text{react}} \rangle \simeq 1.9 \times 10^{46} f_{PB}^{-1} f_{CL}^{-1} \Xi \left( \frac{M_{DC}}{M_\odot} \right)^{1/3} \left( \frac{\text{yr}}{T} \right) \left( \frac{\text{km}}{a_1} \right)^{5/2} \left( \frac{M_\odot \text{ pc}^{-3}}{\rho_*(0)} \right)^2 \times$$

$$\left\{ \left[ 1 + 2.1 \times 10^{-27} \Xi^{-1} f_{CL} \left( \frac{\rho_*(0)}{M_\odot \text{pc}^{-3}} \right) \left( \frac{T}{\text{yr}} \right) \left( \frac{a_1}{\text{km}} \right)^{3/2} \right]^{5/3} - 1 \right\} \quad (79)$$

Let us now require  $\langle t_{react} \rangle$  to exceed the age of the Universe (taking evidently  $T \simeq 10^{10}$  yr). As it is apparent from eq. (76),  $t_{react}$  is shorter for softer binaries. Hence, in order to contemplate *hard* binaries with an arbitrary orbital radius we have to set  $a_1 \simeq 1.4 \times 10^{12} (M_\odot / M_{DC})^{2/3}$  km in eq. (79). Correspondingly, the binary survival condition reads<sup>19</sup>

$$f_{PB} \lesssim 8.2 \times 10^{-5} f_{CL}^{-1} \Xi \left( \frac{M_{DC}}{M_\odot} \right)^2 \left( \frac{M_\odot \text{pc}^{-3}}{\rho_*(0)} \right)^2 \times \left\{ \left[ 1 + 35 f_{CL} \Xi^{-1} \left( \frac{\rho_*(0)}{M_\odot \text{pc}^{-3}} \right) \left( \frac{M_\odot}{M_{DC}} \right) \right]^{5/3} - 1 \right\}. \quad (80)$$

Although the presence of various dark cluster parameters prevents a clear - cut conclusion to be drawn from eq. (80), in the illustrative case  $M_{DC} \simeq 10^5 M_\odot$  and  $f_{CL} \simeq 0.5$  eq. (80) entails e.g.  $f_{PB} \lesssim 0.3$  for  $\rho_*(0) \simeq 3 \times 10^3 M_\odot \text{pc}^{-3}$ . Thus, we infer that for realistic values of the parameters in question a sizable fraction of primordial binary brown dwarfs survives binary-binary encounters in the dark cluster cores<sup>20</sup>.

## 5 Thermal balance in halo molecular clouds

As far as the energetics of halo molecular clouds is concerned, we can identify two main heat sources. One is energy deposition from background photons, while the other is of gravitational origin (coming from frictional hardening of primordial binary brown dwarfs). Although we shall discuss them separately, it should be kept in mind that they both act at the same time.

<sup>19</sup>Application of the same argument to tidally - captured binaries shows that no depletion occurs in this way.

<sup>20</sup>If the initial value of  $f_{PB}$  fails to satisfy condition (80), primordial binaries start to be destroyed in binary-binary encounters until their fractional abundance gets reduced down to a value consistent with condition (80).

## 5.1 Energy from background photons

We proceed to estimate  $T_m$  by momentarily neglecting gravitational effects. To this end, we need to know the heating rate (due to external sources) and the cooling rate (due to the molecules). In the galactic halo, the dominant heat source for molecular clouds is expected to be ionization from photons of the X-ray background, whose spectrum in the relevant range  $1 \text{ keV} < E < 25 \text{ keV}$  (see below) can be parametrized in terms of the energy  $E$  (expressed in keV) as  $I(E) = 8.5 E^{-0.4} \text{ cm}^{-2} \text{ s}^{-1} \text{ sr}^{-1}$  (O’Dea et al. [1994]). The ionization rate per  $H_2$  molecule (taking secondary ionization into account) is

$$\xi_X = 26 \int_{E_{min}}^{E_{max}} 4\pi I(E) \sigma_X(E) dE \text{ s}^{-1}, \quad (81)$$

where  $\sigma_X(E) = 2.6 \times 10^{-22} E^{-8/3} \text{ cm}^2$  is the absorption cross-section in the above energy range for incoming X-rays on gas with interstellar composition (Morrison and McCammon [1983]). Actually,  $\sigma_X(E)$  decreases faster as  $E$  increases when the gas metallicity is lower (see Fig.1 in Morrison and McCammon [1983]). So, the above quoted expression for  $\sigma_X(E)$  is expected to yield an upper bound on the cross-section for X-rays on halo molecular clouds. The integration limits  $E_{min}$  (below which X-rays are absorbed) and  $E_{max}$  (above which X-rays go through the whole cloud without being absorbed) depend on the cloud column density. Thus, taking as an orientation  $n_m$  in the range  $10^4 - 10^8 \text{ cm}^{-3}$ , we get  $1.25 \text{ keV} < E_{min} < 7 \text{ keV}$  and  $10 \text{ keV} < E_{max} < 20 \text{ keV}$ . It turns out that  $\xi_X$  is rather insensitive to the upper limit, and we obtain  $\xi_X = 2.2 \times 10^{-19} \text{ s}^{-1}$

for  $E_{min} = 1.25 \text{ keV}$  and  $\xi_X = 5.6 \times 10^{-21} \text{ s}^{-1}$  for  $E_{min} = 7 \text{ keV}$  <sup>21</sup>. Since

<sup>21</sup> It is straightforward to verify that the ionization rate  $\xi_{cr}$  due to the halo cosmic rays is less important in this context. In fact, assuming the ionization rate per  $H_2$  molecule typical for disk cosmic rays  $\xi_0 = 5 \times 10^{-17} \text{ s}^{-1}$  (see e.g. van Dishoeck and Black [1986]) and rescaling for the diffusion of the cosmic rays in the galactic halo (De Paolis et al. [1995b]), we infer  $\xi_{cr} \sim 10^{-23} \text{ s}^{-1}$ .

each ionization process releases an energy of  $\simeq 8$  eV, the heating rate per  $H_2$  molecule  $\Gamma$  turns out to be

$$3.5 \times 10^{-32} \text{ erg s}^{-1}/H_2 < \Gamma < 1.5 \times 10^{-30} \text{ erg s}^{-1}/H_2 . \quad (82)$$

Unfortunately, the cooling rate for the halo clouds in question is not well known, owing to the lack of detailed information on their chemical composition. Nevertheless, by merely considering the cooling rate due to  $H_2$  as given by Goldsmith and Langer [1978], the equality between cooling and heating rate per molecule leads to  $T_m \simeq 10$  K. More complete models for the cooling rate, which include the contribution from  $HD$  and heavy molecules, imply that the cooling efficiency is substantially enhanced and thus make it very plausible that halo molecular clouds clumped into dark clusters should have a temperature close to that of the CBR, namely  $T_m \simeq 3$  K (see also Gerhard and Silk [1996] for similar conclusions).

## 5.2 Energy from primordial binary brown dwarfs

As the analysis in Sect 4.3 shows, dynamical friction transfers a huge amount of energy from primordial binary brown dwarfs to molecular clouds, and so it looks compelling to investigate (at least) the gross features of the ensuing energy balance.

Let us start by evaluating the energy acquired by molecular clouds in the process of frictional hardening. Recalling that the traversal time for a single cloud is given by eq. (61), eq. (58) entails that – after a binary with initial orbital radius  $a_1$  has crossed  $N$  clouds – its orbital radius gets reduced down to

$$a_{N+1} \simeq \left[ 1.1 \times 10^{-19} N \Xi^{-1} \left( \frac{\text{pc}}{r_m} \right) \left( \frac{M_\odot}{M_{DC}} \right)^{1/3} + \left( \frac{\text{km}}{a_1} \right)^{3/2} \right]^{-2/3} \text{ km} . \quad (83)$$

Accordingly, we see that the orbital radius remains almost constant until  $N$  reaches the critical value

$$N_0 \equiv 9 \times 10^{18} \Xi \left( \frac{r_m}{\text{pc}} \right) \left( \frac{M_{DC}}{M_\odot} \right)^{1/3} \left( \frac{\text{km}}{a_1} \right)^{3/2}, \quad (84)$$

whereas it *decreases* afterwards. Because the energy acquired by the clouds is just the binding energy given up by primordial binaries, this information can be directly used to compute the energy  $\Delta E_c(N)$  gained by the  $N$ -th cloud traversed by a binary whose initial orbital radius was  $a_1$ . Manifestly, we have

$$\Delta E_c(N) = \frac{1}{2} G m^2 \left( \frac{1}{a_{N+1}} - \frac{1}{a_N} \right). \quad (85)$$

Thanks to eq. (83), a straightforward calculation shows that  $\Delta E_c(N)$  stays practically constant

$$\Delta E_c \simeq 9.8 \times 10^{32} \Xi^{-1} \left( \frac{\text{pc}}{r_m} \right) \left( \frac{M_\odot}{M_{DC}} \right)^{1/3} \left( \frac{a_1}{\text{km}} \right)^{1/2} \text{ erg}, \quad (86)$$

as long as  $N \lesssim N_0$ , while it subsequently *decreases*. So, the amount of energy transferred to a cloud is maximal during the early stages of hardening. Now, since the binding energy of a cloud is

$$E_c \simeq 7.7 \times 10^{42} \left( \frac{r_m}{\text{pc}} \right) \text{ erg}, \quad (87)$$

it can well happen that  $\Delta E_c > E_c$  (depending on  $r_m$ ,  $M_{DC}$  and  $a_1$ ), which means that the cloud would evaporate unless it manages to efficiently dispose of the excess energy.

A deeper insight into this issue can be gained as follows (we focus the attention on the early stages of hardening, when the effect under consideration is more dramatic). Imagine that a spherical cloud is crossed by a primordial binary which moves along a straight line, and consider the cylinder  $\Delta$  traced by

the binary inside the cloud (its volume being approximately  $\pi a^2 r_m$ ). Hence, by  $n_m \simeq 62.2 (\text{pc}/r_m)^2 \text{ cm}^{-2}$  (which follows from eq. (12)) the average number of molecules inside  $\Delta$  turns out to be

$$N_\Delta \simeq 5.8 \times 10^{30} \left( \frac{a_1}{\text{km}} \right)^2 \left( \frac{\text{pc}}{r_m} \right). \quad (88)$$

Physically, the energy  $\Delta E_c$  gets first deposited within  $\Delta$  in the form of heat. Neglecting thermal conductivity (more about this, later), the temperature inside  $\Delta$  accordingly becomes

$$T_\Delta \simeq \frac{2}{3} \frac{\Delta E_c}{N_\Delta k_B} \simeq 8.1 \times 10^{17} \Xi^{-1} \left( \frac{M_\odot}{M_{DC}} \right)^{1/3} \left( \frac{\text{km}}{a_1} \right)^{3/2} \text{ K}, \quad (89)$$

$k_B$  being the Boltzmann constant. On account of eqs. (40) and (72), eq. (89) yields

$$0.5 \Xi^{-1} \left( \frac{M_{DC}}{M_\odot} \right)^{2/3} \text{ K} \lesssim T_\Delta \lesssim 16.2 f_{CL} \Xi^{-2} \left( \frac{\rho_*(0)}{M_\odot \text{pc}^{-3}} \right) \left( \frac{M_\odot}{M_{DC}} \right)^{1/3} \text{ K}, \quad (90)$$

which – in the illustrative case  $f_{CL} \simeq 0.5$ ,  $\rho_*(0) \simeq 3 \times 10^3 M_\odot \text{pc}^{-3}$  and  $M_{DC} \simeq 10^5 M_\odot$  – entails in turn  $5.3 \times 10^3 \text{ K} \lesssim T_\Delta \lesssim 1.3 \times 10^4 \text{ K}$ . As a consequence of the increased temperature, the molecules within  $\Delta$  will radiate, thereby reducing the excess energy in the cloud. In order to see whether this mechanism actually prevents the cloud from evaporating, we notice that the characteristic time needed to accumulate the energy  $\Delta E_c$  inside  $\Delta$  is just the traversal time  $t_m$ . Therefore, this energy will be totally radiated away provided the cooling rate per molecule  $\Lambda$  exceeds the critical value  $\Lambda_0$  given by the equilibrium condition

$$N_\Delta \Lambda_0 t_m \simeq \Delta E_c. \quad (91)$$

Specifically, eq. (91) yields

$$\Lambda_0 \simeq 10^{-12} \Xi^{-1} \left( \frac{\text{pc}}{r_m} \right) \left( \frac{\text{km}}{a_1} \right)^{3/2} \text{ erg s}^{-1} \text{ mol}^{-1}, \quad (92)$$

on account of eqs. (61), (86) and (88). Moreover, in the present case in which most of the molecules are  $H_2$  the explicit form of  $\Lambda$  is (see e.g. O’Dea et al. 1994, Neufeld et al. 1995)

$$\Lambda \simeq 3.8 \times 10^{-31} \left( \frac{T_\Delta}{\text{K}} \right)^{2.9} \text{ erg s}^{-1} \text{ H}_2^{-1} , \quad (93)$$

which - thanks to eq. (89) - becomes

$$\Lambda \simeq 3.4 \times 10^{21} \Xi^{-2.9} \left( \frac{\text{km}}{a_1} \right)^{4.35} \text{ erg s}^{-1} \text{ H}_2^{-1} \quad (94)$$

(notice that  $\Lambda$  is almost independent of  $M_{DC}$ ). Now, from eqs. (92) and (94) it follows that the condition  $\Lambda \gtrsim \Lambda_0$  implies

$$a_1 \lesssim 6 \times 10^{11} \Xi^{-0.7} \left( \frac{r_m}{\text{pc}} \right)^{0.35} \text{ km} . \quad (95)$$

For a wide range of dark cluster and molecular cloud parameters it turns out that eq. (95) is fulfilled for hard primordial binaries.

Thus, we conclude that the energy given up by primordial binary brown dwarfs and temporarily acquired by molecular clouds is efficiently radiated away, so that the clouds do not get dissolved by frictional hardening.

As a final comment, we stress that our estimate for  $T_\Delta$  should be understood as an upper bound, since thermal conductivity has been neglected. In addition, the above analysis implicitly relies upon the assumption  $T_\Delta < 10^4$  K, which ensures the survival of  $H_2$ . Actually, in spite of the fact that condition (90) entails that this may well not be the case, our conclusion remains nevertheless true. For, higher temperatures would lead to the depletion of  $H_2$ , which correspondingly gets replaced by atomic and possibly ionized hydrogen. As is well known, in either case the resulting cooling rate would exceed the one for  $H_2$ , and so cooling would be even more efficient than estimated above (Böhringer & Hensler 1989).

## 6 Lyman- $\alpha$ absorption systems

It is well known that Quasar Ly- $\alpha$  absorption lines provide a detailed information on the evolution of the gaseous component of galaxies (see e.g. Fukugita, Hogan and Peebles [1996] and references therein). These lines are seen for a neutral hydrogen column density  $N_{HI}$  ranging from  $\sim 3 \times 10^{12} \text{ cm}^{-2}$  (the detection threshold) to  $\sim 10^{22} \text{ cm}^{-2}$ .

At the upper limit of this range ( $N_{HI} \geq 2 \times 10^{20} \text{ cm}^{-2}$ ) the lines are classified as damped Ly- $\alpha$  systems (mostly associated with metal-rich objects) and it is generally believed that they are the thick progenitors of galactic disks. The  $HI$  distribution in damped Ly- $\alpha$  systems is usually flatter than the corresponding surface brightness of the optical disks and extends to much larger radii (up to  $\sim 40 \text{ kpc}$  in giant galaxies). In the outer galactic regions Ly- $\alpha$  systems show sharp  $HI$  edges at a level of  $N_{HI} \sim 10^{17} \text{ cm}^{-2}$ , the so-called Lyman limit. Damped Ly- $\alpha$  systems are observed up to redshift  $z \sim 3.5$  and the survey results suggest that the average mass of neutral hydrogen per absorption system decreases with time, in agreement with the hypothesis of gas consumption into stars (Lanzetta, Wolfe and Turnshek [1995]).

Within our picture, it is tempting to identify damped Ly- $\alpha$  systems with the PGC clouds in the inner galactic halo, where they undergo disruption.

Below the Lyman limit (i.e. for  $3 \times 10^{12} \text{ cm}^{-2} < N_{HI} < 3 \times 10^{15} \text{ cm}^{-2}$ , see e.g. Fig. 2 in Cristiani [1996]), the absorption lines are classified as Ly- $\alpha$  forest and are generally ascribed to a large number of intervening clouds (in some cases extending up to  $\sim 200 \text{ kpc}$  from a central galaxy) along the line of sight to distant Quasars. Studies of Ly- $\alpha$  forest lines have made rapid progress recently and some observational trends are today firmly established. In particular: (i)



The evolution of the co-moving number density of systems per unit interval in redshift shows that the number of Ly- $\alpha$  forest clouds rapidly decreases with time for  $z > 2$ , while it is approximately constant for  $z < 2$ . (ii) The correlation between the thermal Doppler parameter  $b$  and the number of clouds can be fitted with a gaussian distribution of median  $\langle b \rangle \simeq 30 \text{ km s}^{-1}$  and dispersion  $\simeq 10 \text{ km s}^{-1}$ , corresponding to a temperature of a few  $10^4 \text{ K}$ .

Within our model, it looks natural to identify Ly- $\alpha$  forest clouds with the molecular clouds clumped into dark clusters located in the outer halo. Indeed, we expect that the clouds contain in their external layers an increasing fraction of  $HI$  gas and that the outer regions are even ionized, due to the incoming UV radiation <sup>22</sup>. Observe that so far we have been assuming that halo molecular clouds have a constant temperature. This was a good approximation as far as the previous analysis was concerned, but would be too poor in the present discussion. A  $HI$  column density of  $\sim 10^{14} \text{ cm}^{-2}$  – corresponding to a layer of about  $10^{-6} \text{ pc}$  – is sufficient to shield the incoming radiation. Remarkably enough,  $N_{HI} \sim 10^{14} \text{ cm}^{-2}$  corresponds to the average value of the observed Lyman- $\alpha$  forest distribution (Cristiani [1996]). Since we expect the UV flux to decrease as the galactocentric distance increases, clouds which lie at a larger distance may thus have a smaller  $HI$  column density, whereas clouds closer to the galactic disk may have a higher column density. This fact explains the observed distribution for the column density. Moreover, the number of clouds is expected to decrease with time initially, due to both MACHO and  $H_2$  formation, in this way explaining the observed evolution of Ly- $\alpha$  forest clouds according

---

<sup>22</sup>Observe that so far we have been assuming that halo molecular clouds have a constant temperature. This was a good approximation as far as the previous analysis was concerned, but would be too poor in the present discussion

to the above-mentioned point (*i*). As a final comment, we mention that very recently Röttgering, Miley and Van Ojik [1996], by considering the filling factors and the physical parameters derived from their Ly- $\alpha$  forest observations, pointed out that galactic halos may contain  $\sim 10^9 M_{\odot}$  of neutral hydrogen gas and are typically composed of  $\sim 10^{12}$  clouds, each of size  $\sim 40$  light-days. It looks remarkable that these are the typical parameters of molecular clouds dealt with in this paper.

A thorough quantitative analysis requires, however, further investigations, which are beyond the scope of the present paper.

## 7 Conclusions

Looking back at what we have done, it seems to us fair to say that present-day results of microlensing experiments towards the LMC are amenable of a very simple explanation in terms of what was repeatedly proposed as a natural candidate for baryonic dark matter, namely brown dwarfs. Once this idea is accepted, a few almost obvious steps just follow. First, given the fact that ordinary halo stars form in (globular) clusters, it seems more likely that brown dwarfs as well form in clusters rather than in isolation (this circumstance has been repeatedly recognized in the last few years). Of course, whether brown dwarfs are still clumped into dark clusters today is a different and nontrivial question – we have seen that core collapse can liberate a considerable fraction of brown dwarfs from the less massive dark clusters. Second, much in the same way as it happens for ordinary stars, a consistent fraction of binary brown dwarfs (up to 50% in mass) is expected to form. Third, since no known star-formation mechanism is very efficient, it is natural to imagine that a substantial amount

of primordial gas is left over. Although we cannot be sure about the subsequent fate of this gas – which should be mostly cold  $H_2$  – it is likely to remain confined within the dark clusters, since stellar winds are absent. So, also cold  $H_2$  self-gravitating clouds should presumably be clumped into dark clusters, along with some residual diffuse gas.

We have shown that – within the considered model – not too hard primordial binary brown dwarfs turn out to have an orbital radius which is typically of the order of the Einstein radius for microlensing towards the LMC. Therefore, they are not so easily resolvable in the microlensing experiments performed so far, but we argue that they can be resolved in future microlensing experiments with a more accurate photometric observation <sup>23</sup>, the signature being small deviations from standard microlensing light curves (Dominik [1996]). Notice that such a procedure complements the detection strategy for binaries suggested by Gaudi and Gould [1997].

Many physical processes certainly occur in the dark clusters, and the (likely) presence of a large amount of gas makes them even more difficult to understand than globular clusters. Moreover, the lack of any observational information makes any attempt to figure out the physics of dark clusters almost impossible, were it not for some remarkable structural analogies with globular clusters that the model – upon which our discussion is based – naturally suggests. What should anyway be clear is that a host of different phenomena can happen. Some of them have intentionally been neglected here, in order not to make the present paper either excessively long or too speculative. Yet, many others are likely to

---

<sup>23</sup> See e.g. the ongoing experiments by the GMAN and PLANET collaborations (Proceedings of the *Second International Workshop on Gravitational Microlensing Surveys*, Orsay, 1996).

occur, that we have not even been able to imagine.

## 8 Acknowledgements

We would like to thank B. Bertotti, B. Carr and F. D'Antona for useful discussions. FDP has been partially supported by the Dr. Tomalla Foundation and by INFN. FDP and GI acknowledge some support from ASI (Agenzia Spaziale Italiana).

## References

- [1996] Adams, F.C. & Laughlin, G. 1996, ApJ 468, 586
- [1993] Alcock, C. et al. 1993, Nat 365, 621
- [1997] Alcock, C. et al. 1997, ApJ 486, 697
- [1990] Ashman, K. M. 1990, MNRAS 247, 662
- [1962] Antonov, V. A. 1962, Vestn Leningrad-Gross. Univ. 7, 135
- [1993] Aubourg, E. et al. 1993, Nat 365, 623
- [1994] Bahcall, J., Flynn, C., Gould, A., & Kirhakos, S. 1994, ApJ 435, L51
- [1984] Bettwieser, E. & Sugimoto, M. 1984, MNRAS 208, 439
- [1987] Binney, J. & Tremaine, S. 1987 *Galactic Dynamics* Princeton University Press, Princeton
- [1989] Böhringer, H. & Hensler, G. 1989, A&A 215, 147
- [1989] Burrows, A., Hubbard, W. B. & Lunine, J. I. 1989, ApJ 345, 939

- [1994] Carr, B. 1994, *Ann. Rev. Astron. Astrophys.* 32, 531
- [1984] Carr, B. J., Bond, J. & Arnett, W. 1984, *ApJ* 277, 445
- [1987] Carr, B. J. & Lacey, C. G. 1987, *ApJ* 316, 23
- [1996] Chabrier, G., Segretain, L. & Méra, D 1996, *ApJ* 468, L21
- [1995] Charlot, S. & Silk, J. 1995, *ApJ* 445, 124
- [1980] Cohn, H. 1980, *ApJ* 242, 765
- [1984] Cohn, H. & Hut, P. 1984, *ApJ* 277, L45
- [1996] Cristiani, S. 1996, ESO preprint 1117
- [1972] Dalgarno, A & McCray, R. A. 1972, *ARAA* 10, 375
- [1987] D'Antona, F. 1987, *ApJ* 320, 653
- [1995a] De Paolis, F., Ingresso, G., Jetzer, Ph. & Roncadelli, M. 1995a, *Phys. Rev. Lett.* 74, 14
- [1995b] De Paolis, F., Ingresso, G., Jetzer, Ph. & Roncadelli, M. 1995b, *A&A* 295, 567
- [1995c] De Paolis, F., Ingresso, G., Jetzer, Ph., Qadir, A. & Roncadelli, M. 1995c, *A&A* 299, 647
- [1995d] De Paolis, F., Ingresso, G., Jetzer, Ph. & Roncadelli, M. 1995d, *Comments on Astrophys.* 18, 87
- [1996] De Paolis, F., Ingresso, G. & Jetzer, Ph. 1996, *ApJ* 470, 493
- [1991] De Rújula, A., Jetzer, Ph. & Massó, E. 1991, *MNRAS* 250, 348

- [1992] De Rújula, A., Jetzer, Ph. & Massò, E. 1992, A&A 254, 99
- [1990] Dickey, J. M. & Lockman, F. J. 1990, ARAA, 28, 215
- [1996] Dominik, M. 1996, Thesis, Dortmund University
- [1991] Einaudi, G. & Ferrara, A. 1991, ApJ 371, 571
- [1996] Evans, N.W. 1996, to appear in *Aspects of dark matter in astro and particle physics*, ed. by Klapdor-Kleingrothaus, H. V. (World Scientific, Singapore)
- [1975] Fabian, A. C., Pringle, J. E. & Rees, M. J. 1975, MNRAS 172, 15
- [1994] Fabian, A.C. & Nulsen, P.E.J. 1994, MNRAS 269, L33
- [1985] Fall, S. M. & Rees, M. J. 1985, ApJ 298, 18
- [1996] Fields, B. D., Mathews, G. & Schramm, D. N. 1996, astro-ph 9603035
- [1996] Fukugita, M., Hogan, C. J. & Peebles, P. J. E. 1996, Nat 381, 489
- [1996] Gates, E.J., Gyuk, G. & Turner, M. 1996, Phys. Rev. D53, 4138
- [1997] Gaudi, B.S. & Gould, A. 1997, ApJ 482, 83
- [1996] Gerhard, O. E. & Silk, J. 1996, ApJ 472, 34
- [1997] Gibson, B.K. & Mould, J.R. 1997, ApJ 482, 98
- [1978] Goldsmith P. F. & Langer, W. D. 1978, ApJ 222, 881
- [1996] Graff, D. S. & Freese, K. 1996, ApJ 456, L49
- [1975] Heggie, D. C. 1975, MNRAS 173, 729

- [1989] Heggie, D. C. & Ramamani, N. 1989, MNRAS 237, 757
- [1969] Hénon, M. 1969, A&A 2, 151
- [1994] Hu, E. M., Huang, J. S., Gilmore, G. & Cowie, L. L. 1994, Nat 371, 493
- [1996] Jetzer, Ph. 1996, Helv. Phys. Acta 69, 179
- [1990] Kang, H., Shapiro, P. R., Fall, S. M. & Rees, M. J. 1990, ApJ 363, 488
- [1996] Kawaler, S. D. 1996, ApJ 467, L61
- [1996] Kerins, E. J. 1996, astro-ph 9610070
- [1997] Kerins, E. J. 1997, astro-ph 9704179
- [1995] Lanzetta, K. M., Wolfe, A. M. & Turnshek, D. A. 1995, ApJ 440, 435
- [1990] Larson, R.B. 1990, in *Dynamics and Interactions of Galaxies* ed. Wielen, R. (Springer, Berlin)
- [1986] Lee, H. M. & Ostriker, J. P. 1986, ApJ 310, 176
- [1968] Lynden-Bell, D. & Wood, R. 1968, MNRAS 138, 495
- [1994] Maoz, E. 1994, ApJ 428, L5
- [1996] Metcalf, R. B. & Silk, J. 1996, ApJ 464, 218
- [1979] Miller, G.E. & Scalo, J.M. 1979, ApJS 41, 513
- [1995] Moore, B. & Silk, J. 1995, ApJ 442, L5
- [1983] Morrison, R. & McCammon, D. 1983, ApJ 270, 119
- [1989] Murray, S. D. & Lin, D. N. C. 1989, ApJ 339, 933

- [1995] Nakajima, T. et al. 1995, Nat 378, 463
- [1995] Neufeld, D.A., Lepp, S. & Melnick, G.J. 1995, ApJS 100, 132
- [1997] Nulsen, P.E.J. & Fabian, A.C. 1997, submitted to MNRAS
- [1994] O'Dea, C. P. et al. 1994, ApJ 422, 467
- [1985] Ostriker, J. P., Statler, T. S. & Lee, H. M. 1985, Bull.A.A.S. 16, 946
- [1983] Palla, F., Salpeter, E. E. & Stahler, S. W. 1983, ApJ 271, 632
- [1988] Palla, F & Stahler, E. E. 1988, in *Galactic and Extragalactic Star Formation*, ed. by R.E. Pudeitz and M. Fich, NATO ASI Ser. C **232** (Kluwer Academic Publishers, Dordrecht, 1988) p. 519.
- [1990] Persic, M. & Salucci, P. 1990, MNRAS 247, 349
- [1994] Pfenniger, D., Combes, F. & Martinet, L. 1994, A&A 285, 79
- [1977] Press, W.H. & Teukolsky, S.A. 1977, ApJ 213, 183
- [1996] Quinlan, G. D. 1996, New Astronomy 1, 35
- [1995] Rebolo, R., Zapatero Osorio, M. R. & Martin, E. L. 1995, Nat 377, 129
- [1997] Renault, C. et al. 1997, A&A 324, L69
- [1996] Röttgering, H., Miley, G. & Van Ojik, R. 1996, The Eso Messenger No. 83, 26
- [1990] Ryu, M., Olive, K. & Silk, J. 1990, ApJ 353, 81
- [1997] Sackett, P. D. 1997, ApJ 483, 103



- [1996] Saumon, D. et al. 1996, ApJ 460, 993
- [1985] Scalo, J. M. 1985, in *Protostars and planets II*, ed. by D. C. Black and M. S. Mathews (University of Arizona Press, Tucson, 1985), p. 201
- [1969] Spitzer, L. 1969, ApJ 158, L139
- [1987] Spitzer, L. 1987, *Dynamical Evolution of Globular Clusters*, Princeton University Press, Princeton
- [1971] Spitzer, L & Hart, M. H. 1971, ApJ 164, 399
- [1980] Spitzer, L & Mathieu, R. D. 1980, ApJ 241, 618
- [1972] Spitzer, L. & Thuan, T. X. 1972, ApJ 175, 31
- [1987] Statler, T. S., Ostriker, J. P & Cohn, H. N. 1987, ApJ 316, 626
- [1985] Stodolkiewicz, J. S. 1985, IAU Symposium 113, *Dynamics of Star Clusters*, ed. Goodman, J. & Hut, P. (Reidel, Dordrecht)
- [1990] Tamanaha, C. M., Silk, J., Wood, M. A. & Winget, D. E. 1990, ApJ 358, 164
- [1996] Unavane, M., Wyse, R. & Gilmore, G. 1996, MNRAS 278, 727
- [1986] van Albada, T. S. & Sancisi, R. 1986, *Phil. Trans. R. Soc. London A* 320, 447
- [1986] van Dishoeck, E. F. & Black, J. H. 1986, ApJS 62, 109
- [1995] Vietri, M. & Pesce, E. 1995, ApJ 442, 618
- [1977] Zahn, J. P. 1977, A&A 57, 383